

Review of current advances in the mechanical description and quantification of aortic dissection mechanisms

Joseph Brunet^{1,*}, Baptiste Pierrat¹, and Pierre Badel¹

¹Mines Saint-Etienne, Univ Lyon, Univ Jean Monnet, INSERM, U 1059 Sainbiose, Centre CIS, F - 42023 Saint-Etienne France

*Corresponding author: joseph.brunet@emse.fr

Abstract—Aortic dissection is a life-threatening event associated with a very poor outcome. A number of complex phenomena are involved in the initiation and propagation of the disease. Advances in the comprehension of the mechanisms leading to dissection have been made these last decades thanks to improvements in imaging and experimental techniques. However, the micro-mechanics involved in triggering such rupture events remains poorly described and understood. It constitutes the primary focus of the present review. Towards the goal of detailing the dissection phenomenon, different experimental and modeling methods were used to investigate aortic dissection, and to understand the underlying phenomena involved. In the last ten years, research has tended to focus on the influence of microstructure on initiation and propagation of the dissection, leading to a number of multiscale models being developed. This review brings together all this material in an attempt to identify main advances and remaining questions.

KEYWORDS: arterial dissection, aorta, mechanical failure, mechanisms, initiation

I. INTRODUCTION

The largest artery in the body, the aorta, is the most prone to dissection, a mechanical failure event with very serious consequences. Though well described clinically, the conditions and mechanisms initiating this life-threatening event are partially described and known to limited extent, making dissection a poorly understood vascular incident. The present review aims at bringing together current knowledge and material addressing this essential problematic, in order to highlight possible relevant future directions for research in this field.

The aorta is composed of three layers. The innermost layer is the intima. It is composed of (i) a single and smooth layer of endothelial cells in contact with blood, called endothelium, underlying on (ii) a thin basal membrane (~ 80 nm) and (iii) a sub-endothelial layer composed of smooth muscle cells, collagenous bundles and elastic fibrils [1], [2]. Subendothelial layer thickness depends on location,

age and disease. Although the endothelium does not contribute significantly to the mechanical behavior of the arterial wall, the subendothelial layer certainly does. Holzapfel et al. [3] demonstrated that in coronary arteries the subendothelial layer exhibits a significant thickness, load-bearing capacity, and mechanical strength in comparison with the media and adventitia. The middle layer is the media. It is a complex structure consisting in several lamellar units called musculo-elastic fascicles, separated by elastin laminae. Each unit is mainly composed of elastin, type I and III collagen and smooth muscle cells [4], [5]. The media is separated from the intima by the internal elastic lamina and from the adventitia by the external elastic lamina. Due to its organization, similar to laminate composites, the media resists to relatively high loads in longitudinal and circumferential directions but is weaker in the radial direction [6]; hence, it is prone to dissection separation, a delamination event. The outermost layer is the adventitia. It is composed mainly of fibroblasts, fibrocytes, ground substance and type I collagen [5]. It is surrounded by connective tissue and the limit between the two is not clearly defined. The vasa vasorum, a network of vessels and capillaries in the adventitia and outer part of the media, provides blood supply and nourishment to the aortic wall. The adventitia has a significant role in the stability and ultimate strength of the artery. At the unloaded state, adventitial collagen is crimped, the consequence is that the media mainly contributes to the mechanical behavior of the arterial wall at low pressure. However, at a significant strain, collagen fibers are straightened and the arterial wall becomes extremely stiff, effectively preventing the artery from overstretching and rupture. Furthermore, the arterial wall is not stress-free without external loads, layer-specific residual stresses were evidenced [7] and shown to play an important role as pointed out by Holzapfel et al. [8]. In particular, it may homogenize the circumferential stress, thus diminishing the stress gradients through the aortic wall.

Aortic dissection is a sudden delamination of the aortic wall occurring in the medial layer. In the majority of cases, dissection is described as initiating with an intimal tear which then allows blood flowing in the media [9], although intramural haemorrhage can also lead to dissection [10], [11] (Figure 1). Aortic dissection most often occurs in the ascending aorta, along the right lateral wall, where the maximum shear stress caused by blood flow is located [12]. Another common site is below the ligamentum arteriosum, in the descending thoracic aorta [13], [14]. The dissection can propagate either in the antegrade or retrograde direction from the intimal tear or haemorrhage. Once the intimal entry (or tear) is formed, propagation starts, eventually creating an intimal flap. Two pathways for the blood are then present, the true lumen and the false lumen. This condition is extremely dangerous for the patient as it affects the mechanical integrity of the arterial wall, compromising its strength and hemodynamics due to the false lumen narrowing the true lumen, or occluding collateral vessels, which leads to a decrease in blood supply of tissues and organs.

Aortic dissection requires rapid diagnosis and decision-making. The incidence of this pathology is 35 cases per 100,000 people per year among the 65–75 years of age. Risk factors include hypertension, atherosclerosis and genetic disorders that affect connective tissue like Marfan syndrome [12]. Without intervention, up to 90% of patients with acute aortic dissection die within weeks [15]. Aortic dissection can also be caused by traumas, for instance occurring in a car accident [12], or during catheter insertion [16], [17]. For example, balloon angioplasty can lead to several undesirable side effects including permanent damaging of the arterial wall caused by over-stretch and atherosclerotic plaque fracture [18].

Because its immediate consequences are hemodynamics-related, existing aortic dissection was often studied from the perspective of fluid mechanics and fluid-structure interactions [19], the objective of such approaches being to determine which treatment would be the most appropriate for a given patient, with minimum potential complications. Various approaches were applied to investigate the effect of hemodynamics on aortic dissection. Thanks to advances in medical imaging such as 4D magnetic resonance imaging (MRI), blood flow velocity [20], [21] and arterial wall displacement [22] can be measured during the cardiac cycle which constitutes valuable input for such approaches. However, the accuracy is still not sufficient to assess the wall shear stress accurately [23], especially in aortic dissection where flow velocity gradients around the dissection are high, and the presence of an intimal flap makes it even more complex. To address this issue, computational fluid dynamics approaches coupled

with patient-specific models were used [24]–[27]. These models allowed obtaining local pressure and wall shear stress values. Yet, some assumptions on which they rely are questionable. A major one is to consider the aortic wall as rigid, while it is very compliant and its geometric variations may be substantial. A relevant approach, in that respect, is fluid-structure interaction modeling [28]–[30] which couples fluid and solid mechanics. Though very promising, these models involve many constitutive and numerical parameters, in addition to intrinsic complexity (example: remeshing issues when large transformations occur) [31]. Although the results of such investigations are crucial to improve clinical care and help in decision making for patients suffering from an already detected dissection, models related to hemodynamics will not be reviewed in this paper. Readers are referred to the work of Morris et al. [32] for further reading on these aspects.

The mechanical event of aortic dissection itself can be separated in two different mechanisms: initiation and propagation, the causes and most influential factors of which are not well understood. Rajagopal et al. [33] postulated that initiation of the aortic dissection can be related to systolic blood pressure, while pulse pressure and heart rate can influence its propagation. Osada et al. [34] observed that most aortic dissections developed in the outer third of the media, alongside the vasa vasorum, suggesting an important role of the vasa vasorum in initiation of aortic dissection. Recently, pooling of glycosaminoglycans/proteoglycans was identified as a possible cause for aortic dissection initiation by creating significant stress concentrations and intra-lamellar swelling in the arterial wall [35]–[37].

The various conclusions and hypotheses formulated based on these studies reveal a marked lack of understanding of the underlying mechanisms involved in aortic dissection initiation and propagation certainly due to the complexity and multiple causes involved. In particular, advanced mechanical analyses of the underlying mechanisms based on mechanical experiments, as well as structural observations at the relevant scales combining mechanical loading and imaging, would deeply improve current knowledge of these life-threatening events and could improve clinical decision criteria. In this context, the objective of the present review is to focus on previous works which address relevant aspects to these questions of initiation and propagation of aortic dissection. An overview of the experimental techniques will be addressed first. Then, modeling approaches will be presented along with their added value and limitations. This review will be concluded by open questions and perspectives.

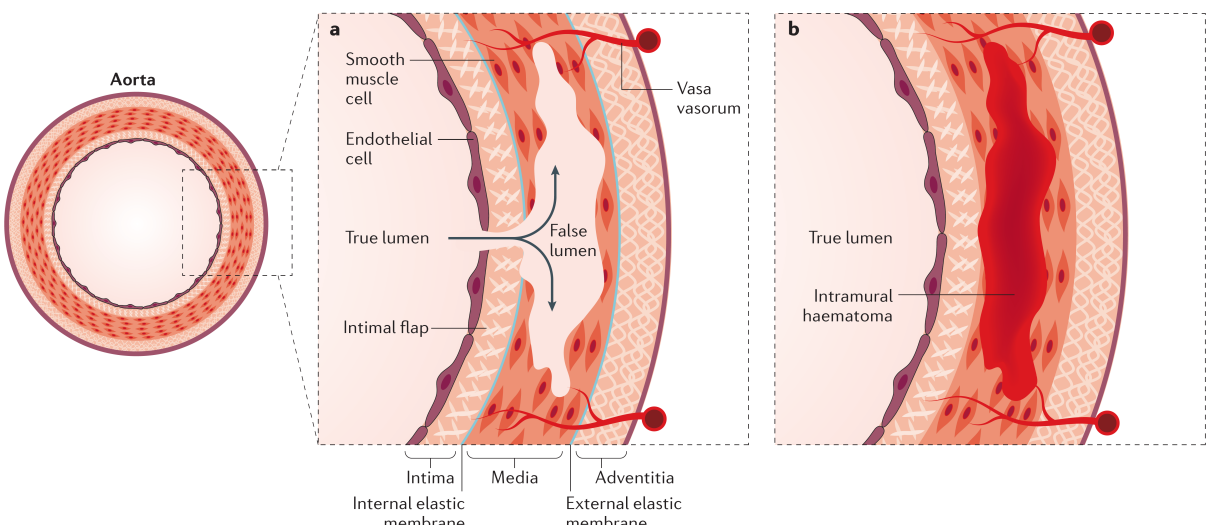


Figure 1: Aortic dissection propagating in the medial layer of the aortic wall. (a) An intimal tear is present and allows the blood to flow in the media creating a false lumen. (b) In some cases, an intramural haematoma caused by a rupture in the vasa vasorum can also progress in dissection. Reproduced from Nienaber et al. [12].

II. EXPERIMENTAL APPROACHES TO DISSECTION MECHANICS

Aortic dissection is a complex vascular event involving several phenomena at different scales. Experimental studies focusing on the mechanisms behind this phenomenon are still rare in the literature. A likely reason is that aortic dissection, and especially its initiation, is a dynamic, transient process which turns out to be difficult to observe or quantify due to its spontaneity and relative short duration. In addition, the complexity of the vascular wall micro-structure explains the difficulty of identifying the modes of rupture involved in aortic dissection.

In this regard, it must be mentioned that imaging techniques have been a prerequisite to any progress towards improved management and understanding of dissection. On both clinical and research sides, available imaging techniques present advantages and drawbacks, requiring compromises to be made according to each use. Acquisition time, field of view, resolution are typical features of interest in this context. Imaging techniques are essential to most of the research presented in this review but all technical aspects and choice-making criteria are out of the present scope. Only a brief overview of the most common techniques, used in clinics and/or research works detailed herein, is provided in Table I. It should be emphasized that this comparison was made from a research point of view and not from a clinical one.

Animal tissues are extensively used for in-vitro mechanical testing (Section II-A), although human tissue has also been characterized. Porcine aortic tissue is usually regarded as a good candidate due to its anatomical similarity, although not identical [60], with human

aortic wall [61]. However, the majority of porcine aortas are harvested on young healthy animals while aortic dissection occurs in cases of medial degeneration and hypertension [62]. On the other hand, mouse models have been widely used for in-vivo testing, as detailed in section II-B.

In the following, we report the work of several authors who performed experimental investigations aiming at describing and quantifying the mechanisms involved in aortic dissection. In brief, macro-scale investigations mainly provided global descriptive trends on dissection propagation, as well as quantitative energetic values involved in the delamination phenomena. On the other hand, experiments performed at lower scales were relevant in addressing more quantitative aspects related to elementary mechanisms possibly involved in the dissection sequence from initiation to a propagated dissection, towards a possible classification of these mechanisms. This section is divided into two parts, addressing respectively *in vitro* and *in vivo* investigations.

A. *In vitro* characterizations

Fracture can happen following three modes: mode I is described by a normal opening with respect to the crack surface, mode II is described by shear sliding parallel to the crack surface but orthogonal to the leading edge, and mode III is described by shear sliding parallel to the crack surface and to the leading edge (Figure 2). These modes can be mixed depending on, for instance, the external loading, the material properties, and the crack propagation. Though mode I is very likely to be dominant in an already opened dissection which propagates due to blood pressure, a detailed

Imaging Technique	Spatial Resolution	Field of view	Advantages	Drawbacks	References
Clinical Computed Tomography (CT)*	$\sim 500 \mu\text{m}$	Non limiting	Widely available	Contrast agent needed Ionizing radiation	[38]–[40]
Clinical MRI*	$\sim 1 \text{ mm}$	Non limiting	Great scale of view Good contrast	Long-time scan Lack of availability	[38], [41]
Clinical Echocardiography techniques*	$\sim 100 \mu\text{m}$	Maximum depth: 100 mm	Great temporal resolution Portable Cheap	Operator-dependent	[42], [43]
Light-based histology	$0.2 \mu\text{m}$	In plane: $\sim 10 \text{ mm}$	Good resolution Wall scale	Tissue damaged	[44]
Electron-based histology	$\sim 5 \text{ nm}$	In plane: $\sim 10 \mu\text{m}$	Extremely good resolution	Tissue damaged	[45]–[47]
High-resolution Ultrasound	$30 - 100 \mu\text{m}$	Maximum depth: 15 mm; lateral: $\sim 20 \text{ mm}$	Great temporal resolution Good field of view	Poor resolution	[48]–[51]
Multiphoton microscopy	$15 - 1000 \text{ nm}$	Maximum depth: $\sim 300 \mu\text{m}$; lateral: $\sim 750 \mu\text{m}$	Great resolution Intrinsic fluorescence of tissues	Limited field of view Poor penetration	[47], [52], [53]
X-ray computed tomography	$0.150 - 4 \mu\text{m}$	$\sim 1\text{-}10 \text{ mm}^3$	Good field of view Great resolution	Ionizing radiation Contrast agent needed	[54]–[57]
Optical coherence tomography	$1 - 10 \mu\text{m}$	Maximum depth: 5 mm; lateral: $\sim 1 \text{ mm}$	Great resolution	Shadowing effect Poor penetration Low contrast	[52], [58], [59]

* Representative equipment used in standard clinical practices

Table I: Comparison of the different imaging techniques currently used in clinics and research. Values present in this table are given as orders of magnitude of what can be accomplished with standard methods, lower resolutions can be achieved in special conditions. Spatial resolution and field of view correspond to a range of values found in the mentioned references for imaging arterial tissue.

and accurate description of fracture modes and their ratios from early initiation to complete propagation of dissection remains an open question. The present subsection introduces studies that were performed to characterize these fracture modes in the context of arterial dissection.

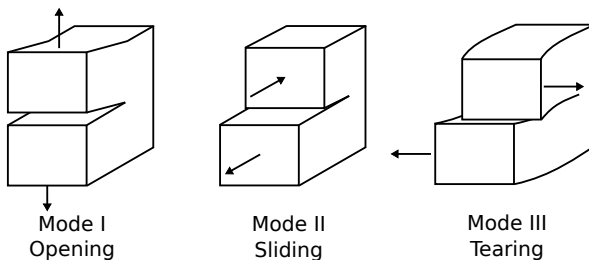


Figure 2: The three fracture modes: opening mode (mode I), sliding mode (mode II), and tearing mode (mode III).

1) *Liquid infusion test:* One of the first techniques used to study the mechanisms leading to dissection was developed by Roach and co-workers. A fluid was infused at a constant flow rate into the media using a thin needle, resulting in the progressive delamination of elastic laminae in the path of least resistance, while recording pressure and volume. In an early study, Carson et al. [63] assessed the strength of the media and its influence on the propagation of the dissection thanks to this technique. The test was done on 31 opened porcine upper descending thoracic aortas. The peak pressure to tear the aortic media was $77.2 \pm 1.5 \text{ kPa}$ (579 mmHg) which is a non-physiological blood pressure suggesting that the mechanical strength of the aortic wall has to be weakened for aortic dissection to initiate. The energy release rate required to propagate the dissection was $15.9 \pm 0.9 \text{ mJ/cm}^2$, and the pressure required to propagate the dissection dropped down to a physiological range, which suggests

a clear distinction between initiation and propagation events. Tiessen et al. [64] investigated the influence of several parameters on the propagation of dissection in 21 opened unpressurized human aortas. The peak pressure to tear the media was $79 \pm 29 \text{ kPa}$ and their results did not show any significant effect of age and tear depth on medial strength of human aorta. However, sex, location and atherosclerotic plaque formation did. Roach et al. [65] studied the influence of the location on the energy required to propagate the dissection in 17 opened porcine aortas. The energy release rates were $2.84 \pm 1.19 \text{ mJ/cm}^2$ for the upper thoracic aorta, $2.90 \pm 1.21 \text{ mJ/cm}^2$ for the lower thoracic aorta, $1.88 \pm 0.89 \text{ mJ/cm}^2$ for upper abdominal aorta and $11.34 \pm 4.05 \text{ mJ/cm}^2$ for lower abdominal aorta. It was also observed that the lower abdominal aorta tore at a lower pressure but required higher energy to propagate the dissection. Observations with scanning electron microscopy (SEM) suggested a change in the elastin microstructure between the thoracic aorta and the abdominal aorta. This could explain the difference in values. Using the same technique, but with pressurized aortas under static conditions (i.e. no flow), Tam et al. [66] investigated the influence of tear depth on the propagation of the dissection in porcine thoracic aorta. Blebs were created in the media using saline solution and a circumferential slit was made on the intimal side to connect the true and false lumen. Then, the aortas were pressurized under no-flow conditions until propagation. Their results showed that propagation of the dissection occurred for tear (normalized) depth of 0.44 to 0.89 (with 1 being closest to the adventitial side). A positive correlation was found between the propagation pressure and the number of medial units remaining in the dissected wall. Conversely, but logically, inverse correlation was found between the propagation pressure and the tear depth.

These correlations were not found in the previously detailed studies [63], [64] which may be explained by differences in the experimental methods and/or tissues.

2) Radial tensile test: An intuitive way to approach the mechanisms underlying aortic dissection is radial tensile testing aimed at directly studying medial separation. This mechanical test gives an indication about the interlamellar connection strength in the aortic wall, which is relevant in dissection propagation because it is likely to be driven by mode I fracture properties. To prepare the specimens for radial tensile test, the artery is opened longitudinally and a rectangular or cylindrical sample is cut out. Sandpaper and glue are commonly used to fix the sample in the testing machine and avoid slippage in the clamps. Maclean et al. [6] compared the response of upper and lower porcine thoracic aorta to radial stresses with the response to longitudinal and circumferential stresses. The elastic modulus was calculated for different values of strain, showing that, just before failing, it is significantly lower in radial direction (61.4 ± 4.3 kPa) than in longitudinal and circumferential directions (112.7 ± 9.2 kPa and 151.1 ± 8.6 kPa). Later, Sommer et al. [67] investigated the strength of the media of 8 human abdominal aortas using the same test. The radial failure stress was 140.1 ± 15.9 kPa. The stress-strain curves were divided in three parts: region S1 for elastic, S2 for damage accumulation and S3 for failure, with the behavior of S1 being linear elastic unlike most biological tissues which exhibit a typical J-shaped curve. Furthermore, a peeling-like mechanism was observed during rupture, showing a lamellar decohesion process (Figure 3). Another more recent study on human thoracic aortic tissue confirmed that the tensile strength could be ranked in decreasing order from circumferential, to longitudinal and radial direction [68]. This result could explain the fact that, once a tear is present, the dissection propagates generally in the tangential plane (either in longitudinal or circumferential direction).

3) Peeling test: Peeling is a mechanical test that was often used to study the propagation of dissection. While tensile tests in radial direction allow assessing the strength between layers of the aortic wall, the peeling test is more appropriate to measure the mode I energy release rate in the separation of layers [69]. To prepare the specimens for such a test, the artery is opened longitudinally and a rectangular strip is cut out. One end of the specimen is, then, split in the thickness to get two tongues that are respectively fixed in each clamp of the testing machine. Sandpaper or glue is also commonly used to avoid slippage in the clamps. A schematic of the experimental setup before and after the test is shown in Figure 4. Force and displacement are measured throughout the test, allowing extraction of the mode I energy release rate

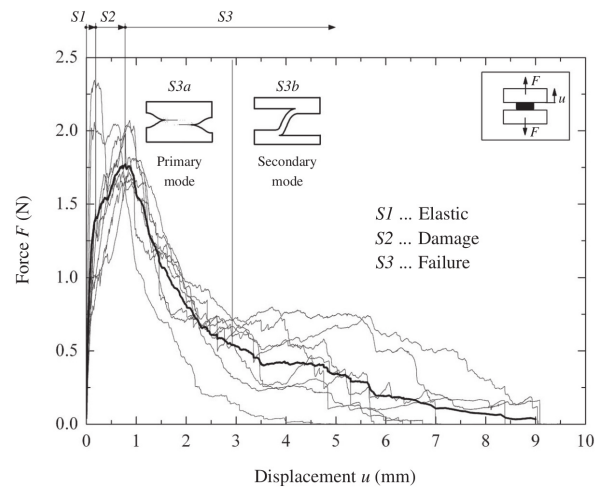


Figure 3: Force-displacement curves, from direct tension tests, of 8 samples of human abdominal aortas, with the thick curve representing the arithmetic mean response. The initial decohesion of the medial layers S3a is followed by a peelinglike failure mechanism S3b. Reproduced from Sommer et al. [67].

(involved in dissection propagation). The advantage of peeling tests mainly lies in the control of fracture propagation, unlike direct tension tests or inflation tests where fracture is unstable. Sommer et al. [67] analyzed the dissection properties of the media of 12 human abdominal aortas using peeling tests. The dissection energy release rates were 5.1 ± 0.6 mJ/cm² in the circumferential direction and 7.6 ± 2.7 mJ/cm² in the longitudinal direction. This indicates a possible anisotropy of propagation properties, suggesting a preferred propagation of dissection in the circumferential direction. The authors suggested that, from a structure-to-mechanics point of view, this may be explained by the anisotropic arrangement of the different components like elastin, collagen fibers and smooth muscle cells, which may impact the fracture response as it does for the elastic response of such tissue. This is supported by the fact that peeling in the longitudinal direction generated a "rougher" surface compared to peeling in the circumferential direction. It is also interesting to note that the crack of the medial dissection was observed to spread over six or seven elastic laminae, hence not being confined to the same lamellae when propagating. Tong et al. [70] used the same methodology on 62 human carotid bifurcations to study their dissection behavior. The dissection energy release rate required was lower in circumferential direction than in longitudinal direction and the surface generated by longitudinal peeling tests was "rougher" compared with the surface generated by the tests in the circumferential direction, consolidating the hypothesis of anisotropy of cohesive properties previously observed in Sommer et al. [67]. Also, the measured energy release rate

significantly varied with the location, higher energy is required to propagate a dissection in the common carotid artery than in the internal carotid artery. Pasta et al. [71] used peeling tests to compare the dissection behavior of aneurysmal and non-aneurysmal human ascending thoracic aorta from bicuspid aortic valve (BAV) or tricuspid aortic valve (TAV) patients. The results exhibited a delamination strength significantly greater for non-aneurysmal samples than for aneurysmal samples, regardless of the valve morphology and testing direction. They also showed that, for aneurysmal samples, delamination strength of BAV samples was significantly lower than delamination strength of TAV samples for both directions. This demonstrates that patients with thoracic aneurysm have a greater risk of aortic dissection and that patients with BAV are more prone to aortic dissection than patients with TAV, in qualitative agreement with clinical experience. Considering that several studies reported structural differences between these categories of tissues [72]–[74], this conclusion raises the need to explore and understand the mechanisms involved at the microstructural level. A significant difference was also found between circumferential and longitudinal directions within non-aneurysmal specimens with higher delamination strength in longitudinal direction, like in Tong et al. [70]. However, this significant difference was not observed within aneurysmal specimens which suggested that the delamination behavior of aneurysmal samples was isotropic.

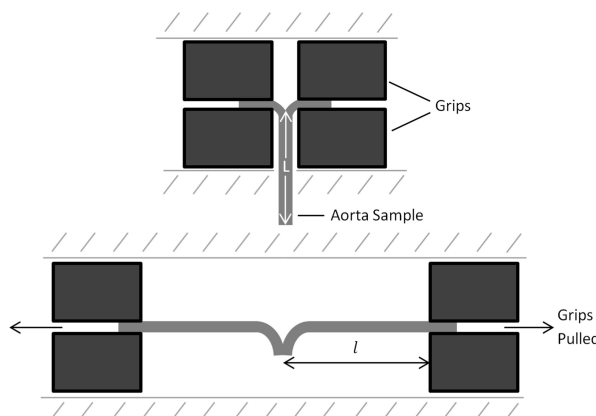


Figure 4: Experimental set up for peeling test, before the test and after the test. Reproduced from Noble et al. [75].

4) Tearing test: Also called trousers test, the tearing test is close to the peeling test in its implementation (the orientation of the sample is simply changed in the testing machine); however, the mechanisms of failure observed may be different as this test allows investigating mode III fracture. Purslow et al. [76] performed this experiment on descending thoracic aortas and showed that the failure stress is greater in the circumferential direction than in the longitudinal direction, and in both

orientations the strength increased further away from the heart. To date, more investigation is necessary to confirm the presence of mode III in aortic dissection.

5) Shear test: Several studies addressed shear testing on arterial wall to find its shear modulus. Vosoughi et al. [77] applied shear deformation on bovine aortic rectangular samples (hence deforming them in a parallelogram-like shape) and derived their shear modulus. Other studies used extension-inflation-torsion tests on human common carotid arteries [78] and porcine coronary artery [79] to also derive the shear modulus. However, these studies did not investigate rupture of the tissue under these testing conditions. In another approach, Haslach et al. [80] drew radial lines on ring-shaped samples of bovine descending aorta and observed that these lines, during inflation of the ring, actually curved due to non-uniform circumferential displacement. Thus the authors concluded that shear stress may arise when inflating the aorta, confirming their earlier finding [81]. To investigate this, shear tests were performed on bovine rectangular aortic wall blocks in longitudinal and circumferential directions. No difference in the shear stress response was found between the two directions but a redistribution of the interstitial fluid due to shear deformation was observed. More interestingly regarding vascular damage, the histology performed in this work revealed growth of local voids within medial tissue along the collagen fibers (Figure 5), indicating inter-fiber crosslink rupture. The increasing number of such voids was hypothesized to favor crack propagation in the arterial wall by connecting them. Furthermore, some bridge-crossing fibers can be seen in Figure 5. The nature of these bridging fibers (collagen, elastin, or both) remains to be clearly identified, as they were designated as elastin fibers in Pasta et al. [71] while they are clearly collagen in Haslach et al. [80] who used collagen staining. Focusing on more relevant and advanced tests for understanding dissection micro-mechanisms, Haslach et al. [80] performed the ring inflation experiment by making an additional radial cut on the intimal side, with the aim of simulating an intimal tear initiating a dissection. Their results showed that the crack first grew in circumferential direction, and eventually this circumferential crack propagation stopped when a radial crack formed and completely broke the sample. Since circumferential crack propagation cannot be induced by circumferential stress or radial compressive stress, this observation suggested that a non-zero shear stress was present during inflation. It was concluded that rupture of the aortic ring in this test involved mode II fracture propagation, probably caused by shearing of inter-fiber crosslinks, and a final rupture due to a mode I radial crack by pull-out or rupture of the collagen fibers. Though this study was performed in the absence

of blood, it questions the influence of shear-driven, hence mode II, effects in dissection. A hypothesis that can be formulated is that the early stages of crack opening would be controlled by mode II properties, while the following propagation would be driven by mode I properties when the blood rushes into the crack. The authors concluded that mode II should be considered with more interest in future research. Haslach et al. [82] inflated healthy bovine aortic rings with an intimal-medial longitudinal tear. The crack propagated in the circumferential direction suggesting that mode II fracture is predominant compared to mode I opening, confirming the precedent results. In order to quantify these shear rupture phenomena, Sommer et al. [68] performed tri-axial shear tests on 16 human thoracic aortas. The tri-axial shear tests were done following the different orientations of the orthotropic microstructure of the aorta. The aortic medial shear strength was found to be higher in the rz -plane and $r\theta$ -plane ('out of plane') than in the $z\theta$ -plane ('in plane'). Furthermore, higher ultimate 'in plane' shear stresses and amounts of shear were found in the longitudinal direction compared to the circumferential direction which denotes an anisotropy of the tissue concerning failure under shear loading. Ultimate 'in plane' shear stresses in the circumferential and longitudinal direction were not significantly different for aneurysmatic tissues, but significantly different for dissected tissues. In addition, uni-axial tensile tests were performed in circumferential, longitudinal and radial directions in the same study. They revealed much lower failure strength under 'in plane' shear loading compared to longitudinal and circumferential tensile strength, suggesting that aortic tissues are weaker against shear stress compared to tensile stress. In a comprehensive study, Witzenburg et al. [83] investigated and quantified the failure behavior of aortic tissue by performing uni-axial, equi-biaxial, peel and shear lap tests on porcine ascending aortas. Uni-axial testing revealed higher strength in the lamellar plane (circumferential and longitudinal direction), while peel and shear lap tests showed a low strength for interlamellar connections (radial direction). Unlike Sommer et al. [68], shear lap tests showed a significantly higher peak stress in circumferential direction (185.4 ± 28.4 kPa) than in longitudinal direction (143.7 ± 16.0 kPa). Note, however, that this difference may be explained by the differences between tests or tissues. The authors noticed that the shear lap failure stress was remarkably lower than the uni-axial failure stress in both longitudinal (753 ± 228 kPa, n=11) and circumferential (2510 ± 979 kPa, n=11) directions, confirming the previous observations in [68].

6) Tension-inflation test: In many *ex vivo* models, a tear was created in an excised sample of aorta, a pulsatile pump mimicked the blood flow, and pressure

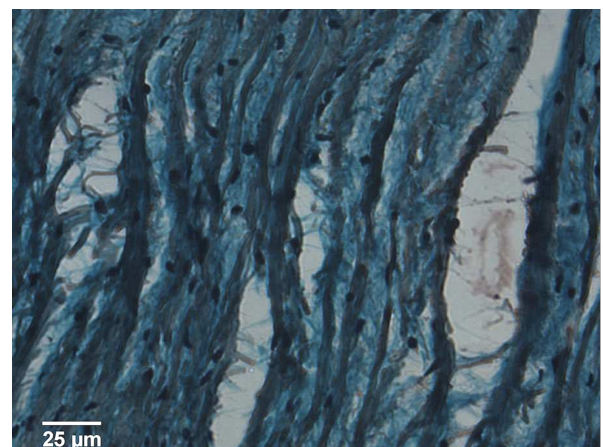


Figure 5: Slice of bovine descending aorta after translational shear test, loaded in the circumferential direction, with $\times 400$ magnification. Voids can be seen between collagen fibers in the medial circumferential-radial plane. Bridges crossing these voids are also visible. The vertical direction is circumferential. The stains used were Fast Green FCF, which stains the collagen green, Safranin O, which stains the proteoglycans and other tissue polyanions reddish, and Hematoxylin, which stains cell nuclei. Reproduced from Haslach et al. [80].

and flow rate were recorded [84]–[87]. In particular, the recent study by Peelukhana et al. [88] investigated the effect of geometric and hemodynamic parameters on the propagation of dissection in descending thoracic porcine aortas. A single entry tear was made inside the samples and a pulsatile pressure setup was used to propagate the dissection. A significant effect of the initial intimal-medial tear geometry (circumference, longitudinal length, and depth) on the dissection propagation was observed. Furthermore, unlike the mean pressure, pulse pressure was found to be the major contributor to flap movement and hence to dissection propagation. Using a similar setup, Prokop et al. [89] and Van Baardwijk et al. [90] both found that $(\frac{dP}{dt})_{max}$ had a significant influence on the dissection propagation in contrast to mean pressure. Based on mathematical reasoning, Rajagopal et al. [33] questioned this conclusion and hypothesized that both pulse pressure and cycle frequency, which are related to $(\frac{dP}{dt})_{max}$, are the main contributors to dissection propagation.

In *ex vivo* models, the procedure to create the initial tear is obviously less complex than in *in vivo* models. Furthermore, the different parameters like location and geometry of the initial tear or pressure and flow rate of the blood flow can be controlled, making this method useful to investigate the influence of these parameters on the propagation of dissection. Another advantage, compared to *in vivo* models, is that human aorta can be studied. However, this type of model was only useful to study propagation of dissection and not the initiation. In addition, the underlying micro-mechanisms could

not be described based on the cited work of this subsection, suggesting the need to develop experiments at lower scales.

7) In situ testing: *In situ* imaging combined with mechanical testing is a promising approach to observe microstructural deformation, and possibly rupture. This allows the identification of underlying phenomena occurring under mechanical loading. Ideally, the sample should be imaged by a 3D non-invasive imaging technique, under physiological conditions [91], thus preventing the use of histology as it alters the mechanical integrity of the sample. With such approaches, all previous tests presented in section II-A could be performed to investigate the respective mechanisms involved and quantify structural descriptors at the relevant scale depending on the imaging technique. Therefore, *in situ* imaging is extremely interesting in the investigation of aortic dissection because it theoretically allows the observation of the initiation sequence and the propagation. The main limitation is the temporal resolution, as aortic dissection is a sudden rupture event. Due to this obstacle, the literature is limited on the application of such method on aortic dissection.

Among possible techniques, X-ray computed tomography is a non-destructive technique widely used in both industrial and medical fields. The principle is based on the attenuation of X-rays by matter and their detection by an X-ray sensor after penetration throughout the opaque sample. Several views are taken at different angles and mathematical methods allow the 3D geometry and the internal structure to be reconstructed. To image soft tissues, a contrast agent is needed to obtain enough contrast with conventional absorption-based equipment [54]. The resolution with this technique can be close to $1 \mu\text{m}$ and the field of view is around 1 mm^3 . However, μ -CT can damage the sample due to radiation induced by the photon beam [92] and this should be kept in consideration and carefully checked. X-ray phase-contrast imaging, derived from the same technique, is also suitable for low contrast tissue and was already used by Walton et al. [56] to achieve sub- μm spatial resolutions. Using absorption-based X-ray tomography, Helfenstein-Didier et al. [55] did *in situ* tensile tests on medial layers of porcine thoracic aorta (Figure 6), with sodium polytungstate as contrast agent, to assess the microstructural deformation and rupture of the samples under tension. The contrast agent allowed to observe lamellar units of the media. The images showed that the medial rupture always starts on the intimal side. Furthermore, the process of damage initiation, delamination and rupture of the media was described. The authors highlighted the importance of intra-lamellar delamination (mode II) and the need for further investigation.

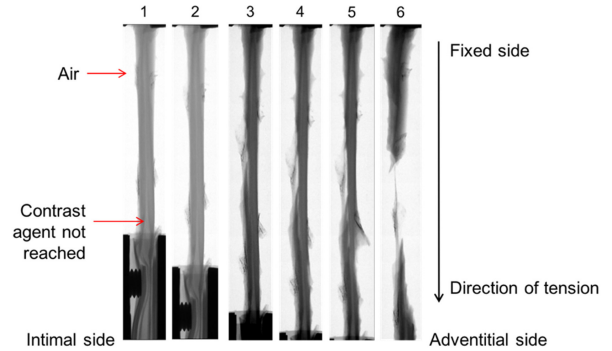


Figure 6: X-ray computed tomography images of a tensile test on a porcine medial sample at different time steps obtained by Helfenstein-Didier et al. [55].

Another *in situ* imaging technique is optical coherence tomography (OCT), it is particularly used in ophthalmology to image transparent media such as retinal tissue and detect the presence of diseases [93]. This technique provides good axial and lateral resolution ($\sim 10 \mu\text{m}$), and better imaging depth ($< 5 \text{ mm}$) than most other optical techniques [52]. Thanks to its high speed acquisition, some studies combined OCT and digital volume correlation during mechanical test to measure the three dimensional deformation fields [58], [94]. Advances in laser field led to μ -OCT, this technique allows the observation of cellular and sub-cellular structure with an axial resolution of $< 1 \mu\text{m}$, a lateral resolution of $< 2 \mu\text{m}$ [95]–[97], and a maximum imaging depth of $500 \mu\text{m}$ [58], [59], making this technique a potential candidate for microstructural investigations in arterial tissue. However, practical implementation for thick non-transparent tissues is not straightforward. A limitation to this technique is that deeper tissue may benefit from less contrast and luminosity due to shadowing effect. Ferruzzi et al. [98] used OCT to observe the passive and active behavior, under biaxial loading, of vulnerable thoracic aortas of mouse models predisposed to aortic dissection, with and without treatment with rapamycin (a macrolide antibiotic and immunosuppressive compound used to coat coronary stent and prevent organ transplant rejection). The authors observed that daily *in vivo* treatment with rapamycin preserved or restored biaxial contractile properties, but not passive properties. The OCT images showed spontaneous *in vitro* delaminations, under physiological loading, in the specimens. In addition, samples from rapamycin-treated mice, tested with induced smooth muscle cell contractility, were all protected against intramural delamination whereas delamination occurred in 55% of the samples after inactivation of smooth muscle cells. In addition, calculations showed that contraction reduced circumferential and longitudinal stresses, suggesting that smooth muscle cell tonus may act as a stress shield for a vulnerable

extracellular matrix.

In recent literature, multiphoton microscopy has been a popular imaging modality to observe the aortic wall structure, however, to the author's knowledge, this technique was never used in conjunction with a mechanical test, in the case of aortic dissection or arterial rupture. The main advantage of multiphoton microscopy is the possibility to use two-photon fluorescence (generated by both elastin and collagen) and second harmonic generation (generated by collagen only) and collect their signals which are easily separable due to their distinctive wavelengths. Hence, it allows imaging collagen and elastin components without any alteration of the sample. Another advantage of this technique is that 3D observation is possible; however maximum depth is around 300 - 600 μm in very best cases, unless optical clearing techniques are used, as was done in Schriefl et al. [99]. Some studies used multiphoton microscopy to observed fibers and characterize tissue morphology (fiber orientation [100], [101], waviness [102], [103], ...) and developed models based on these observations. Several studies also used this image modality to perform *in situ* testing on arterial samples, yet without addressing dissection so far [53], [100], [104], [105]. The main drawback with multiphoton microscopy is that the volume of observation is limited (current limit is approximately 750x750x300 μm^3 , depending on the setup) or that the merging of multiple scans is needed. This limitation may be too restrictive to observe an entire dissection. Also, using a clearing agent to overcome the depth limitation alters the mechanical properties of the tissues due to the dehydration of the sample [106].

In situ imaging methodologies are really promising in the understanding of aortic dissection, especially for the initiation sequence. The choice of the imaging technique is determined as a trade-off between their advantages and drawbacks. X-ray computed tomography has a large field of view but its resolution is not as good as OCT, furthermore, despite its small field of view, multiphoton microscopy can image collagen and elastin fibers without any manipulation of the sample. Hence, future investigations may benefit from methods based on such techniques which seem promising in the understanding of aortic dissection, especially for the initiation sequence.

B. *In vivo characterizations on animal models*

In vivo studies are extremely valuable to understand the evolution of a disease in a physiological environment. Because *in vivo* investigations on human subjects are not possible for obvious ethical reasons, animal models were developed to further our knowledge of the mechanisms behind the initiation and propagation of aortic dissection. Three main types of animal models were commonly used in aortic dissection studies:

drugs- or chemicals-induced, genetically modified, and surgery-induced models. The first and second are used with mice and are of extreme importance to the understanding of aortic dissection underlying phenomena, while the latter can be used with bigger animals and provides a good insight on the effectiveness of aortic dissection treatments over time.

Angiotensin II-infused ApoE $^{-/-}$ mouse is a popular, though not unique, mouse model for aortic aneurysm research [107] but Trachet et al. [108] demonstrated that this model is also suitable for studying aortic dissection. This model induces several microstructural changes like elastin degradation, macrophage infiltration or thrombus formation. Trachet et al. [109] used *in vivo* monitoring and *ex vivo* observation on n=6 controls and n=47 angiotensin II-infused mice. The *in vivo* monitoring was done with high-frequency ultrasound and contrast-enhanced microcomputed tomography after 0, 3, 10, 18 and 28 days of angiotensin II infusion. *Ex vivo* investigation used phase-contrast X-ray tomographic microscopy. These *in vivo* and *ex vivo* observations allowed monitoring the progress of the disease and provided quantitative information about interlamellar hematoma and medial layer ruptures. In particular, the results showed that aortic regurgitation and luminal volume of the ascending aorta significantly increased over time in angiotensin II-infused mice. Furthermore, a significant increase in single laminar ruptures and several focal dissections were observed in the animals. Another classical model used to study aortic dissection is mice infused with β -aminopropionitrile monofumarate (BAPN); it can be combined with angiotensin II to induced the formation of aortic dissections in 100% of the mice [110], [111]. In the same group than Trachet et al. [109], Logge et al. [112] used propagation-based phase-contrast synchrotron imaging to observe n=3 controls and n=10 BAPN/AngII-infused mice after 3, 7 and 14 days of infusion. They were able to reconstruct the complete geometry of murine aortas in 3D with an isotropic voxel size of 1.625 micron, thus quantifying the number of ruptures in medial layers. They also observed that several micro-ruptures developed over time in BAPN/AngII-infused mice and, at a certain moment, connect and create larger tears. This observation suggests a new multi-focal propagation mechanism which would deserve further investigations.

Another type of model, used to investigate the pathogenesis of thoracic aortic disease, is genetically engineered mouse models. For instance, Fbn1 $^{mgR/mgR}$ and Fbn1 $^{C1039G/+}$, two mouse models of marfan syndrome, are widely used. They are obtained by mutation in fibrillin-1 (FBN1) gene and provided advances into the knowledge of molecular pathophysiology mechanisms associated with the onset and the development of the disease as described in the review of Milewicz et

al. [113]. Several other genetically engineered mouse models exist and are used to investigate aortic dissection [114]. Although these models are critical to the understanding of the pathogenesis of this disease, they are not within the scope of this review.

One of the limitations of mouse models is the difference in the number of elastic lamellae in the media, ~7 for mice and ~50 for humans, which may significantly affect the mechanical relevance of the model. Indeed, a medial layer rupture will have a much greater impact on mouse media than human media. However, these models can provide valuable data on the initiation stage of the aortic dissection that can be helpful in the understanding of human aortic dissection.

Another way to create *in vivo* aortic dissection models is surgery, either open surgery or minimally invasive surgery [61], [115], [116]. The principle of these approaches is to create the initial tear in the aorta and propagate the dissection with surgical instruments (Figure 7). Though initiation can obviously not be studied, this procedure has proven to be useful to study the effectiveness over time of several treatments on aortic dissection like stent graft placement or aortic fenestration [117], [118]. However, with this technique, only traumatic dissection due to surgery can be investigated. Other limitations of this procedure are the invasiveness of the method and the difficulty to control the propagation of the dissection, compromising the possibility to extract quantitative data.

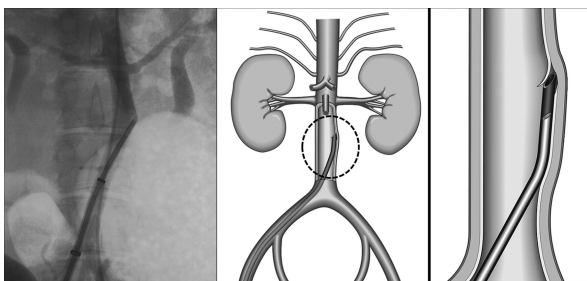


Figure 7: (a) Intraoperative fluoroscopic image showing the tip of a catheter rupturing the abdominal aortic wall. (b) and (c) schematics representing the creation of a surgically induced dissection. Reproduced from Okono et al. [61].

The current state of experimental findings about initiation and propagation of arterial dissection was overviewed in section II. In summary, it should be highlighted that the aortic wall presents an anisotropy in term of tensile strength with a higher ultimate tensile stress in circumferential direction compared to longitudinal direction [68] which may explain why the majority of intimal tears are observed to lie in a radial-circumferential plane, transverse to the longitudinal direction [119]. The aorta also presents an

anisotropic behavior concerning the failure under shear loading [68]. Another observation is that the aortic wall presents a lack of resistance against shear loading compared to tension loading [83]. This may be of uttermost importance considering that Haslach et al. [80] showed that shear stress may be present in the wall during inflation. Fracture mode I and II were investigated in several directions; however, the ratio of each mode in the initiation and propagation of aortic dissection and the mechanisms driving the transition from an initial radial tear, or local medial defect to the crack propagation in the tangential plane of the artery remain unclear. This highlights the lack of experimental studies investigating the relationship between microstructure and mechanical response. *In situ* imaging combined with mechanical testing seems promising to observe the early stage of aortic dissection and shed light on the underlying phenomena driving aortic dissection.

III. MODELS

Although arterial dissection is a challenging phenomenon with many open scientific questions, models trying to investigate dissection are rather scarce in the literature. This is likely due to the fact that aortic dissection is a complex process involving several phenomena at different scales, requiring several assumptions to be made and thus affecting their relevance and potential use.

A. Macro-scale models

The initiation of aortic dissection occurs when the wall stress locally exceeds the tissue's strength. Accordingly, some studies computed the wall stress using finite element analysis and investigated the influence of different parameters on the value and location of peak wall stresses [120], [121], as was often done to assess the rupture risk of aneurysms. The strong assumption behind these studies was that the initiation of dissection is more likely to occur at the peak wall stress location. However, the calculation of this stress was subject to several limitations: the material was considered homogeneous, isotropic, linear elastic and uniform throughout the aorta, with constant thickness. Furthermore, the microstructure of the aortic wall was not taken into account during the construction of the models while it seems to be of high importance in the understanding of aortic wall rupture as peak wall stress was shown to be a poor predictor of the location of rupture [122]. Last, it should be recalled that the relevant measure of stress to be computed in rupture risk assessment remains an open question.

Gasser et al. [123] developed a non-linear continuum framework based on a continuous and a cohesive materials. The continuous material was modeled as a fiber-reinforced composite with collagen fibers embedded

in a non-collageneous isotropic ground matrix, while the cohesive material was represented by a cohesive constitutive law implemented at pre-defined interfaces between adjacent regions of the model. The two materials were independent from each other. The framework was then implemented in a finite element model to reproduce a peeling test and investigate the propagation of arterial dissection. Ferrara et al. [124] presented a numerical model of dissection based on cohesive fracture theory as an evolution of an earlier model applied on the fracture of atherosclerotic plaques [125]. The model was implemented in a numerical finite element simulation of a peeling test (Figure 8 (a)). A sensitivity analysis was then performed to evaluate the influence of the cohesive parameters leading the interlamellar propagation of the dissection in the media and the influence of the reinforcing collagen fibers on the separation of the layers. These simulations suggested that normal and shear strengths played an important role in the separation process, unlike the critical energy release rate. This study highlighted the importance of shear stress in dissection and the need for a failure criterion including the contribution of shear stress. However, the authors underlined that the influence of fiber orientation on shear strength of biological tissues needs further investigation. In addition, this model needs experimental validation. Based on the experimental tests performed by Helfenstein-Didier et al. [55], Brunet et al. [126] confirmed that shear delamination strength between medial layers may contribute to the initiation of aortic dissection by simulating a uni-axial tensile test using a finite element model with cohesive interfaces.

Using finite element method, Wang et al. [128] proposed a computational model to study the propagation of a tear in a fiber-reinforced tissue. An energy-based approach was used by calculating the energy release rate, allowing the identification of the values of pre-existing tear length and internal pressure needed to propagate the tear. The effect of fiber orientation and surrounding connective tissues was also investigated. The model was verified for simple cases, using analytical solutions. The results demonstrated that the presence of fibers reduced the risk of tear propagation, especially when the fibers are parallel to the tear. Nevertheless, decreasing the stiffness of surrounding tissues increased the tear growth. This suggested that connective tissue degeneration leading to softening may facilitate the dissection propagation. Later, in the continuation of their previous works, Wang et al. [127] developed a residually-stressed two-layer arterial model. As previously, the material properties were modelled with Gasser-Holzapfel-Ogden model. The initiation and propagation of the tear were modelled using the extended finite element method, with the behavior of the propagation being described with a

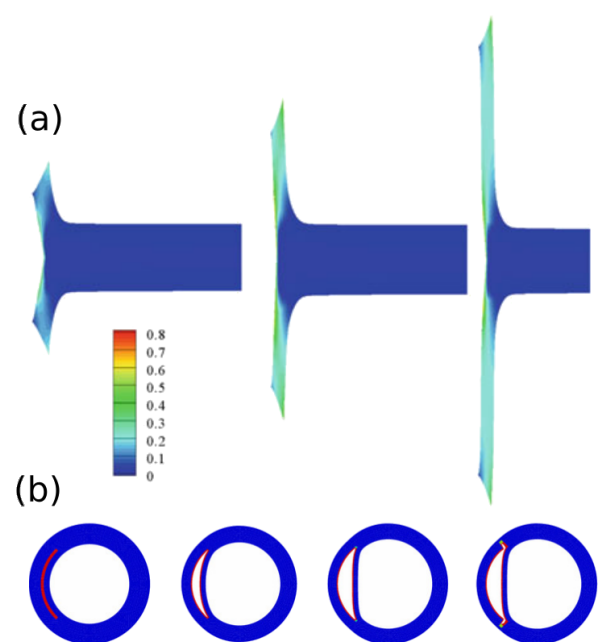


Figure 8: (a) Three different steps of the peeling simulation with the contour level referring to the first principal Cauchy stress in MPa. Reproduced from Ferrara et al. [124]. (b) Evolution of the tear propagation during the inflation of the residually-stressed artery at four different stages. Reproduced from Wang et al. [127].

linear traction-separation law. The study determined the critical pressure at which the dissection started to propagate (Figure 8 (b)). The critical pressure investigated was dimensionless (normalized against the neo-Hookean parameter) and, thus, independent of material properties. Both very short and very long circumferential tears were more stable, meaning that the critical pressure was higher in these cases. Another finding was that longer tears lead to inner wall buckling, as seen on clinical CT scans. Concerning the effect of residual stress, the opening angle increased with the critical pressure, demonstrating that residual stress reduces the risk of propagation. Thus, this model suggests that tear length and residual stress play a key role in the tear propagation. This model was also used in Wang et al. [129] to investigate the influence of several parameters on the dissection propagation by simulating peeling and pressure-loading tests. The main findings were that the tear preferentially propagates along the stiffer direction, which is ruled by the fiber orientation. Furthermore, the model could reproduce various buckling configurations seen on clinical CT images and suggested that a deeper tear is more likely to propagate, confirming that aortic dissection propagates preferentially in the outer third media [34]. This result was also observed experimentally, with different tests, by Tam et al. [66] and Peelukhana et al. [88].

Humphrey and colleagues developed several computational models to examine the influence of medial pooling of glycosaminoglycans on aortic dissection. They demonstrated, using semi-analytical and finite-element-based continuum models, that accumulated glycosaminoglycans may lead to significant intramural stress concentrations and intra-lamellar Donnan swelling pressures [36], [130]. However, damage was not included in these models. Later, Ahmadzadeh et al. [37] developed a particle-based computational model using an extended smoothed particle hydrodynamics (SPH) method. The SPH model was composed of a bi-layered murine aorta. It was verified with a continuum model and validated against experimental data. The purpose of the study was to investigate the role of pooling of glycosaminoglycans in the initiation and propagation of intra-lamellar delamination. The results showed that smooth muscle cell activation can partially prevent damage in the aortic wall, as demonstrated in the literature [98]. The simulations also suggested that close pools of glycosaminoglycans may initiate and propagate a delamination by extending and coalescing.

The models presented in this subsection proved successful to accurately describe aortic dissection behaviour at organ or wall-scale. However, nearly no information about microstructure and associated mechanisms can be obtained with these models apart from the fiber orientation. For a better understanding of the mechanisms behind dissection initiation and propagation, lamellar-scale and micro-scale models are needed (i.e. models where each lamella, or each micro-scale constituent like collagen or elastin fibers is modeled with its own properties). These are presented in the following section.

B. Multi-scale models

Shah et al. [131] presented a computational model combining micro-scale and macro-scale components. The microstructure was modelled as an interconnected fiber network in parallel with a neo-Hookean component that represents the non-fibrous contribution of the extracellular matrix and the smooth muscle cells (Figure 9 (a)). Damage was introduced at the fiber level, with fibers failing when their stretch exceeds a critical threshold. This value was identified, along with elastic parameters, by fitting uni-axial and biaxial extension tests on porcine aortic media. The model was able to reproduce the uni-axial and biaxial responses with good agreement in both pre-failure and failure range. In addition, the model was able to replicate radial tension response from the literature [6] that were not used during the fitting process. The fitted values of the parameters governing the fiber behavior corresponded to elastin fiber rather than collagen fiber, suggesting that elastin is leading the tissue response.

Though it may prove highly valuable for understanding dissection, the lamellar structure of the media is not considered in this model, which is a major limitation. Witzenburg et al. [83] proposed an extension of the previous model, based on histological observations. This time, the microstructure was modelled as a fiber network composed of a 2D sheet of elastin and collagen fibers attached radially by interlamellar connections representing smooth muscle cells and fibrillins. The failure process at the fiber level was maintained from the previous model. This model was able to match the multiple experimental tests (uni-axial, equi-biaxial, peel, and shear lap tests) performed on porcine ascending aorta and agreed well with experiments in the literature. This model constitutes one of the most relevant microstructure-based models currently available. With a similar approach, Thunes et al. [132], [133] used a structural finite element model of the medial lamellar unit including elastic lamellae and collagen fiber network (Figure 9 (b)). The influence of these two load-bearing components on the in-plane tissue strength was investigated, allowing a better understanding of aortic dissection initiation. The model parameters were calibrated using multiphoton microscopy imaging and uni-axial tensile tests in circumferential direction on non-aneurysmal aorta from patient with a normal tricuspid aortic valve, aneurysmal aorta from patients with a tricuspid aortic valve, and aneurysmal aorta from patient with a bicuspid aortic valve. The model was, then, validated against experimental tensile tests in longitudinal direction. According to the results, one of the leading parameter governing tissue strength was the orientation distribution of collagen fibers which controls the fraction of collagen fibers engaged at a given stretch.

Pal et al. [134] based their model on the observations of Pasta et al. [71], and more specifically the increase in peeling force up to a certain value, followed by an oscillation around a plateau value. This demonstrated that delamination does not propagate continuously. An explanation for this phenomenon might be that fibers, present between the layers, create "bridges" between them and support the load induced by delamination. As a portion of fibers breaks, the measured force drops, until new fibers are recruited, allowing the force to increase again. This hypothesis was supported by SEM observations where the authors mentioned a large number of broken elastin fibers in the delamination plane (Figure 10 (a)). In Pal et al. [134], the authors requalified these fibers as collagen and elastin, eventually proposing a predictive mechanistic model that investigated the effect of radially running collagen fibers on the delamination strength (Figure 10 (b)). Using a finite element code, the peel tension response was validated against the results of the tests conducted by Pasta et al. [71]. The model was used to show that

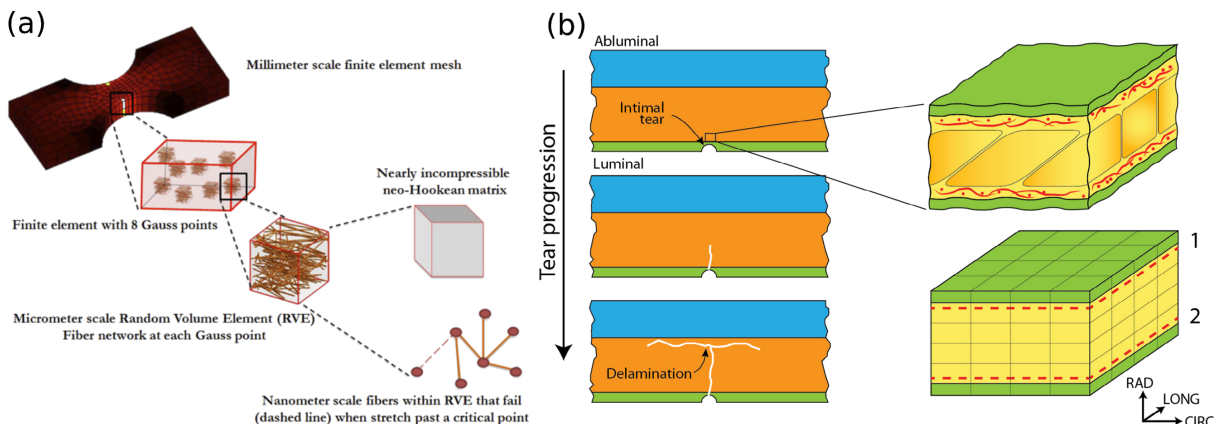


Figure 9: Two examples of multiscale models. (a) Each element of the uni-axial or biaxial finite element geometry is composed of eight Gauss points. These Gauss points consist of representative volume elements (RVE) composed of a fiber network in parallel with a nearly incompressible neo-Hookean matrix. Reproduced from Shah et al. [131]. (b) The model is composed of three layers: the intima (green), media (orange), and adventitia (blue). An intimal tear is present and initiates the aortic dissection (top panel), the tear propagates in the media (middle panel), and delaminates the medial layers (bottom panel). The media consists of several lamellar units, each of them composed of elastic lamellae (green region) and interlamellar space (yellow region). A collagen fiber network (red) is present near the lamellae. Reproduced from Thunes et al. [133].

the density and failure energy of the radially-running collagen fibers were the main contributors to the delamination strength; however, the failure strength of these fibers only affected the initiation of delamination. These findings remain to be confirmed experimentally.

Different models trying to understand the mechanisms of initiation and propagation of aortic dissection were overviewed in this section. Macro-scale models led to several important results for the comprehension of this disease. The importance of shear stress and the need to investigate its influence was highlighted [124], confirming experimental results [80], [83]. Pools of glycosaminoglycans may create significant intramural stress concentrations [36], [130] and play a role in the initiation and propagation of aortic tears [37]. Residual stress and smooth muscle cell activation tend to increase the load bearing capacity of the aortic wall [37], [127]. Furthermore, as demonstrated by experiments [66], [88], a deeper tear is more likely to propagate [129]. These models provided valuable information on aortic dissection mechanisms; however the aortic wall is a complex heterogeneous structure and models at a lower scale are needed to investigate and quantify the influence of the different components. Multi-scale models reproduced different mechanical tests with great accuracy and highlighted the importance of elastin fibers [131] and collagen fibers orientation distribution [133]. The radially-running fibers were investigated by Pal et al. [134] and seem to be of major importance in the propagation of aortic dissection. Unless explicitly mentioned above, the absence of experimental validation remains a limitation and highlights the lack of experimental data on aortic

dissection.

IV. DISCUSSION AND CONCLUSIONS

A number of experimental methods and their results were discussed. These different tests provided qualitative information and quantitative values on the phenomena occurring during aortic dissection. Several questions regarding the pathogenesis and the initiation sequence of the disease remain unanswered. Concerning the initiation sequence, two mechanisms leading to aortic dissection were suggested, originating either from an intimal or intramural tear [12], [135].

The first mechanism is believed to concern the majority of cases: when an intimal tear is present in the aortic wall, this tear will propagate in the outer third of the media, involving about one half of the circumference and creating an aortic dissection [119]. In 85% to 95% of cases, the intimal defect is in the transverse direction, and in a few occurrences in the longitudinal direction [119]. The most common location of intimal tear is a few centimeters above the aortic valve, along the right lateral wall where the shear forces caused by the blood flow are the strongest. The second location of intimal tear is below the ligamentum arteriosum, in the descending thoracic aorta, where the anchoring of the aortic arch with the thoracic cage causes a large increase in stiffness of the arterial wall [13], [135]. As a consequence of the resulting stress or strain state, these areas may be more prone to developing aortic dissections. The origin of intimal tears, or defects that may initiate the dissection, is not well understood, except in the case of injury due to endovascular interventions. This important aspect

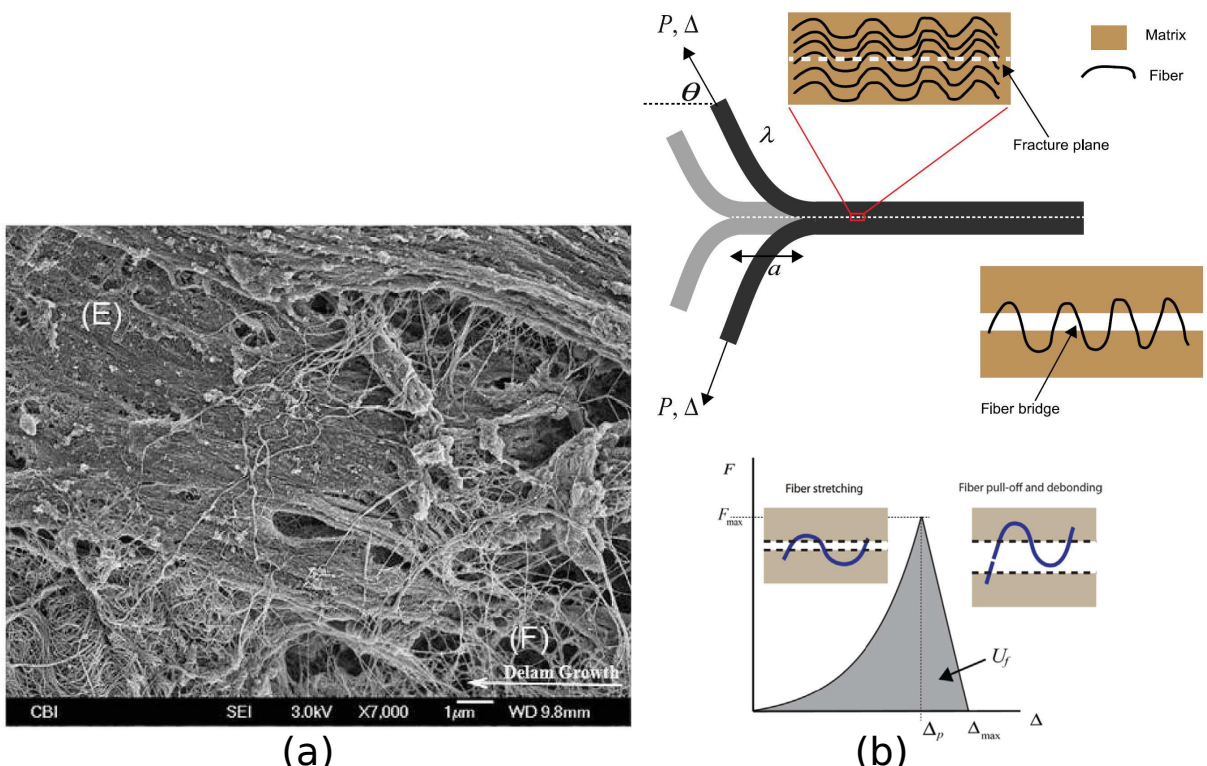


Figure 10: (a) High magnification SEM image of the delamination plane after a peeling test on an ascending thoracic aortic aneurysm with tricuspid aortic valve showing bundles of broken elastic fibers (F) existing between elastic sheets (E). Reproduced from Pasta et al. [71]. (b) Schematic of (1) an artificial dissection, (2) the arrangement of collagen fibers in the fracture plane, (3) a fiber bridge in the delamination plane, and (4) the force-displacement behavior of a collagen fiber. Reproduced from Pal et al. [134].

would also deserve specific research. Nevertheless, it is commonly accepted that a medial degeneration, either from an inherited connective tissue disorder or from an acquired condition compromising the aortic integrity, is fundamental to allow aortic dissection [64], [136], [137]. This degeneration manifests itself by inflammation and extracellular matrix degradation [12], [138], [139]. Hence, mechanical phenomena inducing intimal tears should be investigated in conjunction with biological events that may favor the occurrence of these intimal injuries. For instance, disrupted smooth muscle cell contractility or mechanosensing seems to be the primary driver of aortic dissection [98], [114], [140].

Another essential question concerns the failure modes involved in aortic dissection at the early stage of propagation. Some authors proposed that propagation of an intimal tear is the consequence of a peeling mechanism induced by blood flowing into the defect and pushing the medial layers apart, hence creating a dissection. This scenario involves mode I separation. Another hypothesis is that the intimal tear is propagated by circumferential shear stress, hence involving mode II separation. Haslach et al. [80] hypothesized that shear forces may be present in the arterial wall during the systolic phase suggesting that crack growth

is, at an early stage, driven by internal wall mechanical forces. Supporting this hypothesis, Khanafer et al. [29] demonstrated, thanks to a fluid-structure interaction model, that the peak wall stress and the maximum shear stress are highest in the medial layer. Furthermore, Witzenburg et al. [83] demonstrated the lack of resistance of the aortic media against shear stress compared to uni-axial tensile stress. Thus mode I and II fracture may be the consequence of the intramural mechanical stress induced by the blood flow. More details and evidence are still necessary to clarify these scenarios.

The second mechanism believed to initiate aortic dissection involves an intramural tear, clinically observed in the form of a hematoma due to a rupture of the vasa vasorum [135], [141], [142]. This scenario is supported by the fact that no intimal tear is found in 4% to 12% of aortic dissections [10], [143]–[147]. These non-communicating dissections indicate that an intimal tear is not crucial to initiate aortic dissection. Instead, a weak cohesion of the medial layer would be critical. Khanafer et al. [29] demonstrated that the presence of an intramural hematoma in the aortic wall has a significant effect on the peak wall stress acting on the inner layer, supporting that such a defect can lead

to aortic dissection. Furthermore, it was suggested that intramural hematoma may eventually reach the lumen and create an intimal entry [144]. In this scenario, the intimal tear is secondary to the intramural hemorrhage, as reported in several clinical cases [10], [146], [148], [149]. Thus, intramural hematoma may be the cause of some aortic dissections with intimal flap observed in previous studies. It was also noted in several studies that the vasa vasorum plays a key role in the aortic integrity and that its impairment is followed by mechanical changes resulting in a weakened medial layer [34], [150], [151].

Recent developments in imaging techniques foresee new advances in the understanding of cardiovascular pathologies and especially aortic dissection. The microstructural phenomena are certainly the key to a complete understanding of the initiation and propagation of dissection [152]. Thus, modalities allowing the observation of the microstructure without damaging the sample are crucial. Several techniques seem promising, for instance synchrotron-based X-ray phase-contrast imaging [112] allowing to investigate the microstructure of a sample with a high resolution, on a large field of view while preserving the integrity of the tissue. However, the main challenge to be addressed is to observe a sudden microscopic phenomenon propagating in one or a few seconds [13].

Similar trends were observed with the evolution of modeling approaches, where microstructure is more and more taken into account. Studies combining both experiments and numerical simulation would deeply improve current knowledge. In this context, modeling the medial structure with multiple lamellar units seems unavoidable to determine and quantify the mode of failure involved in aortic dissection. However, a lack of experimental data, in particular on the initiation sequence of aortic dissection, prevents further advances. Such data would be necessary to feed models, and more importantly to validate them.

On this aspect, promising techniques are emerging which could be used to investigate dissection. Zitnay et al. [153] presented a novel method using a collagen hybridizing peptide to optically detect, using fluorescence properties of the peptide, the failure of collagen fibers at the molecular level. With this technique, they were able to track the collagen fiber failure in a rat tail tendon fascicle during a tensile test. In a combined experimental-modelling approach, the same method was used during a tension-inflation test on sheep middle cerebral arteries to investigate the relationship between collagen fiber damage and its impact on the mechanical properties of the tissue [154], [155]. The results showed that the collagen fibers aligned with the direction of loading were the first to damage. More importantly, the authors observed that the tissue-level yielding may be associated with the onset of collagen

damage. This promising technique could be used to detect and follow the initiation sequence of aortic dissection or to quantify the implication of collagen fibers in the different rupture mechanisms.

The understanding of aortic dissection has improved this past decade due to advances in imaging techniques and in computational modeling. Nevertheless, some unknowns remain, especially on the initiation process leading to the propagation of the dissection. Short-term efforts should focus on describing and quantifying the mechanisms involved in the initiation sequence, as well as the relative contribution of each failure mode. The next step will have to involve mechano-biology and remodeling, central issues to later address clinically-relevant matters like the identification of patients at risk, together with the development of clinical decision support tools to address their follow-up and treatments.

V. ACKNOWLEDGEMENTS

This work was supported by the European Research Council through Starting Grant AArteMIS n°638804.

REFERENCES

- [1] J. A. G. Rhodin, "Architecture of the vessel wall," in *Comprehensive Physiology*, R. Terjung, Ed. John Wiley & Sons, Inc., Dec. 1980, pp. 1–31.
- [2] Y. C. Fung, *Biomechanics: mechanical properties of living tissues*. New York: Springer-Verlag, 1993.
- [3] G. A. Holzapfel, G. Sommer, C. T. Gasser, and P. Regitnig, "Determination of layer-specific mechanical properties of human coronary arteries with nonatherosclerotic intimal thickening and related constitutive modeling," *Am. J. Physiol. Heart Circ. Physiol.*, vol. 289, no. 5, pp. H2048–H2058, Nov. 2005.
- [4] J. M. Clark and S. Glagov, "Structural integration of the arterial wall. I. Relationships and attachments of medial smooth muscle cells in normally distended and hyperdistended aortas," *Lab. Invest.*, vol. 40, no. 5, pp. 587–602, May 1979.
- [5] K. von der Mark, "Localization of collagen types in tissues," *Int. Rev. Connect. Tissue Res.*, vol. 9, pp. 265–324, 1981.
- [6] N. F. MacLean, N. L. Dudek, and M. R. Roach, "The role of radial elastic properties in the development of aortic dissections," *J. Vasc. Surg.*, vol. 29, no. 4, pp. 703–710, Apr. 1999.
- [7] C.-J. Chuong and Y.-C. Fung, "Residual stress in arteries," in *Front. Biomed.* Springer, 1986, pp. 117–129.
- [8] G. A. Holzapfel, G. Sommer, M. Auer, P. Regitnig, and R. W. Ogden, "Layer-specific 3D residual deformations of human aortas with non-atherosclerotic intimal thickening," *Ann. Biomed. Eng.*, vol. 35, no. 4, pp. 530–545, Mar. 2007.
- [9] I. Vilacosta, "Acute aortic syndrome," *Heart*, vol. 85, no. 4, pp. 365–368, Apr. 2001.
- [10] C. A. Nienaber, Y. von Kodolitsch, B. Petersen, R. Loose, U. Helmchen, A. Haverich, and R. P. Spielmann, "Intramural hemorrhage of the thoracic aorta: diagnostic and therapeutic implications," *Circulation*, vol. 92, no. 6, pp. 1465–1472, 1995.
- [11] I. Vilacosta, J. A. San Román, J. Ferreirós, P. Aragoncillo, R. Méndez, J. A. Castillo, M. J. Rollán, E. Batlle, V. Peral, and L. Sánchez-Harguindeguy, "Natural history and serial morphology of aortic intramural hematoma: a novel variant of aortic dissection," *Am. Heart J.*, vol. 134, no. 3, pp. 495–507, Sep. 1997.

- [12] C. A. Nienaber, R. E. Clough, N. Sakalihasan, T. Suzuki, R. Gibbs, F. Mussa, M. T. Jenkins, M. M. Thompson, A. Evangelista, J. S. M. Yeh, N. Cheshire, U. Rosendahl, and J. Pepper, "Aortic dissection," *Nat. Rev. Dis. Primers*, vol. 2, p. 16053, Jul. 2016.
- [13] W. C. Roberts, "Aortic dissection: anatomy, consequences, and causes," *Am. Heart J.*, vol. 101, no. 2, pp. 195–214, Feb. 1981.
- [14] D. L. Kasper, Ed., *Harrison's principles of internal medicine*, 19th ed. New York: McGraw Hill Education, 2015.
- [15] N. T. Kouhoukos and D. Dougenis, "Surgery of the thoracic aorta," *N. Engl. J. Med.*, vol. 336, no. 26, pp. 1876–1889, Jun. 1997.
- [16] D. W. Dunning, J. K. Kahn, E. T. Hawkins, and W. W. O'Neill, "Iatrogenic coronary artery dissections extending into and involving the aortic root," *Catheter. Cardiovasc. Interv.*, vol. 51, no. 4, pp. 387–393, Dec. 2000.
- [17] S. Gómez-Moreno, M. Sabaté, P. Jiménez-Quevedo, P. Vázquez, F. Alfonso, D. J. Angiolillo, R. Hernández-Antolín, R. Moreno, C. Bañuelos, J. Escaned, and C. Macaya, "Iatrogenic dissection of the ascending aorta following heart catheterisation: incidence, management and outcome," *EuroIntervention*, vol. 2, no. 2, pp. 197–202, Aug. 2006.
- [18] P. Badel, S. Avril, M. A. Sutton, and S. M. Lessner, "Numerical simulation of arterial dissection during balloon angioplasty of atherosclerotic coronary arteries," *J. Biomech.*, vol. 47, no. 4, pp. 878–889, Mar. 2014.
- [19] B. J. Doyle and P. E. Norman, "Computational biomechanics in thoracic aortic dissection: today's approaches and tomorrow's opportunities," *Ann. Biomed. Eng.*, vol. 44, no. 1, pp. 71–83, 2016.
- [20] Z. Stankovic, B. D. Allen, J. Garcia, K. B. Jarvis, and M. Markl, "4d flow imaging with mri," *Cardiovasc. Diagn. Ther.*, vol. 4, no. 2, p. 173, 2014.
- [21] A. L. Wentland, T. M. Grist, and O. Wieben, "Review of mri-based measurements of pulse wave velocity: a biomarker of arterial stiffness," *Cardiovasc. Diagn. Ther.*, vol. 4, no. 2, p. 193, 2014.
- [22] H. Wang and A. A. Amini, "Cardiac motion and deformation recovery from mri: a review," *IEEE Trans. Med. Imaging*, vol. 31, no. 2, pp. 487–503, 2011.
- [23] J. Szajer and K. Ho-Shon, "A comparison of 4d flow mri-derived wall shear stress with computational fluid dynamics methods for intracranial aneurysms and carotid bifurcations - A review," *Magn. Reson. Imaging*, vol. 48, pp. 62–69, 2018.
- [24] Z. Cheng, F. P. P. Tan, C. V. Riga, C. D. Bicknell, M. S. Hamady, R. G. J. Gibbs, N. B. Wood, and X. Y. Xu, "Analysis of flow patterns in a patient-specific aortic dissection model," *J. Biomech. Eng.*, vol. 132, no. 5, p. 051007, 2010.
- [25] C. Karmonik, J. Bismuth, D. J. Shah, M. G. Davies, D. Purdy, and A. B. Lumsden, "Computational study of haemodynamic effects of entry- and exit-tear coverage in a DeBakey type III aortic dissection: technical report," *Eur. J. Vasc. Endovasc. Surg.*, vol. 42, no. 2, pp. 172–177, Aug. 2011.
- [26] K. M. Tse, P. Chiu, H. P. Lee, and P. Ho, "Investigation of hemodynamics in the development of dissecting aneurysm within patient-specific dissecting atherosclerotic aortas using computational fluid dynamics (CFD) simulations," *J. Biomech.*, vol. 44, no. 5, pp. 827–836, Mar. 2011.
- [27] Z. Sun and T. Chaichana, "A systematic review of computational fluid dynamics in type B aortic dissection," *Int. J. Cardiol.*, vol. 210, pp. 28–31, May 2016.
- [28] F. Gao, Z. Guo, M. Sakamoto, and T. Matsuzawa, "Fluid-structure interaction within a layered aortic arch model," *J. Biol. Phys.*, vol. 32, no. 5, pp. 435–454, 2006.
- [29] K. Khanafar and R. Berguer, "Fluid-structure interaction analysis of turbulent pulsatile flow within a layered aortic wall as related to aortic dissection," *J. Biomech.*, vol. 42, no. 16, pp. 2642–2648, 2009.
- [30] M. Alimohammadi, J. M. Sherwood, M. Karimpour, O. Agu, S. Balabani, and V. Díaz-Zuccarini, "Aortic dissection simulation models for clinical support: fluid-structure interaction vs. rigid wall models," *Biomed. Eng. Online*, vol. 14, no. 1, p. 34, 2015.
- [31] Y. Bazilevs, K. Takizawa, and T. E. Tezduyar, "Challenges and directions in computational fluid-structure interaction," *Math. Models Methods Appl. Sci.*, vol. 23, no. 02, pp. 215–221, 2013.
- [32] P. D. Morris, A. Narracott, H. von Tengg-Kobligk, D. A. Silva Soto, S. Hsiao, A. Lungu, P. Evans, N. W. Bressloff, P. V. Lawford, D. R. Hose, and J. P. Gunn, "Computational fluid dynamics modelling in cardiovascular medicine," *Heart*, vol. 102, no. 1, pp. 18–28, Jan. 2016.
- [33] K. Rajagopal, C. Bridges, and K. R. Rajagopal, "Towards an understanding of the mechanics underlying aortic dissection," *Biomech. Model. Mechanobiol.*, vol. 6, no. 5, pp. 345–359, Aug. 2007.
- [34] H. Osada, M. Kyogoku, M. Ishidou, M. Morishima, and H. Nakajima, "Aortic dissection in the outer third of the media: what is the role of the vasa vasorum in the triggering process?" *Eur. J. Cardiothorac. Surg.*, vol. 43, no. 3, pp. e82–e88, Mar. 2013.
- [35] J. D. Humphrey, "Possible mechanical roles of glycosaminoglycans in thoracic aortic dissection and associations with dysregulated transforming growth factor- β ," *J. Vasc. Res.*, vol. 50, no. 1, pp. 1–10, 2013.
- [36] S. Roccabianca, G. A. Ateshian, and J. D. Humphrey, "Biomechanical roles of medial pooling of glycosaminoglycans in thoracic aortic dissection," *Biomech. Model. Mechanobiol.*, vol. 13, no. 1, pp. 13–25, Jan. 2014.
- [37] H. Ahmadzadeh, M. Rausch, and J. Humphrey, "Particle-based computational modelling of arterial disease," *J. R. Soc. Interface*, vol. 15, no. 149, p. 20180616, 2018.
- [38] E. Lin and A. Alessio, "What are the basic concepts of temporal, contrast, and spatial resolution in cardiac CT?" *J. Cardiovasc. Comput. Tomogr.*, vol. 3, no. 6, pp. 403–408, 2009.
- [39] W. Huda and R. B. Abrahams, "X-ray-based medical imaging and resolution," *Am. J. Roentgenol.*, vol. 204, no. 4, pp. W393–W397, 2015.
- [40] D. T. Ginat and R. Gupta, "Advances in computed tomography imaging technology," *Annu. Rev. Biomed. Eng.*, vol. 16, pp. 431–453, 2014.
- [41] H. Greenspan, "Super-resolution in medical imaging," *The Computer Journal*, vol. 52, no. 1, pp. 43–63, 2008.
- [42] E. L. Meredith and N. D. Masani, "Echocardiography in the emergency assessment of acute aortic syndromes," *Eur. J. Echocardiogr.*, vol. 10, no. 1, pp. i31–i39, 2009.
- [43] C. M. Moran, S. D. Pye, W. Ellis, A. Janeczko, K. D. Morris, A. S. McNeilly, and H. M. Fraser, "A comparison of the imaging performance of high resolution ultrasound scanners for preclinical imaging," *Ultrasound Med. Biol.*, vol. 37, no. 3, pp. 493–501, 2011.
- [44] J. D. Bancroft, *Theory and Practice of Histological Techniques*. Elsevier Health Sciences, Jan. 2008, google-Books-ID: Dhn2KispfdQC.
- [45] A. M. Glauert, "The high voltage electron microscope in biology," *J. Cell Biol.*, vol. 63, no. 3, p. 717, 1974.
- [46] M. K. O'Connell, S. Murthy, S. Phan, C. Xu, J. Buchanan, R. Spilker, R. L. Dalman, C. K. Zarins, W. Denk, and C. A. Taylor, "The three-dimensional micro-and nanostructure of the aortic medial lamellar unit measured using 3D confocal and electron microscopy imaging," *Matrix Biol.*, vol. 27, no. 3, pp. 171–181, 2008.
- [47] A. R. Kherlopian, T. Song, Q. Duan, M. A. Neimark, M. J. Po, J. K. Gohagan, and A. F. Laine, "A review of imaging techniques for systems biology," *BMC Syst. Biol.*, vol. 2, no. 1, p. 74, 2008.
- [48] E. Filoux, J. Mamou, O. Aristizábal, and J. A. Ketterling, "Characterization of the spatial resolution of different high-frequency imaging systems using a novel anechoic-sphere phantom," *IEEE Trans. Ultrason. Ferroelectr. Freq. Control*, vol. 58, no. 5, 2011.
- [49] B. Trachet, R. A. Fraga-Silva, F. J. Londono, A. Swillens, N. Stergiopoulos, and P. Segers, "Performance comparison

- of ultrasound-based methods to assess aortic diameter and stiffness in normal and aneurysmal mice,” *PLoS One*, vol. 10, no. 5, p. e0129007, 2015.
- [50] B. Martin-McNulty, J. Vinclette, R. Vergona, M. E. Sullivan, and Y.-X. Wang, “Noninvasive measurement of abdominal aortic aneurysms in intact mice by a high-frequency ultrasound imaging system,” *Ultrasound Med. Biol.*, vol. 31, no. 6, pp. 745–749, 2005.
- [51] C.-C. Huang, P.-Y. Chen, P.-H. Peng, and P.-Y. Lee, “40 mhz high-frequency ultrafast ultrasound imaging,” *Med. Phys.*, vol. 44, no. 6, pp. 2185–2195, 2017.
- [52] W. Goth, J. Lesicko, M. S. Sacks, and J. W. Tunnell, “Optical-Based Analysis of Soft Tissue Structures,” *Annu. Rev. Biomed. Eng.*, vol. 18, no. 1, pp. 357–385, Jul. 2016.
- [53] C. Cavinato, C. Helfenstein-Didier, T. Olivier, S. R. Du Roscoat, N. Laroche, and P. Badel, “Biaxial loading of arterial tissues with 3D *in situ* observations of adventitia fibrous microstructure: a method coupling multi-photon confocal microscopy and bulge inflation test,” *J. Mech. Behav. Biomed. Mater.*, vol. 74, pp. 488–498, 2017.
- [54] M. Nierenberger, Y. Rémond, S. Ahzi, and P. Choquet, “Assessing the three-dimensional collagen network in soft tissues using contrast agents and high resolution micro-CT: application to porcine iliac veins,” *C.R. Biol.*, vol. 338, no. 7, pp. 425–433, Jul. 2015.
- [55] C. Helfenstein-Didier, D. Taïnoff, J. Viville, J. Adrien, É. Maire, and P. Badel, “Tensile rupture of medial arterial tissue studied by X-ray micro-tomography on stained samples,” *J. Mech. Behav. Biomed. Mater.*, vol. 78, pp. 362–368, Feb. 2018.
- [56] L. A. Walton, R. S. Bradley, P. J. Withers, V. L. Newton, R. E. Watson, C. Austin, and M. J. Sherratt, “Morphological characterisation of unstained and intact tissue micro-architecture by x-ray computed micro-and nano-tomography,” *Sci. Rep.*, vol. 5, p. 10074, 2015.
- [57] E. L. Ritman, “Current status of developments and applications of micro-ct,” *Annu. Rev. Biomed. Eng.*, vol. 13, pp. 531–552, 2011.
- [58] V. A. Acosta Santamaría, M. Flechas García, J. Molimard, and S. Avril, “Three-dimensional full-field strain measurements across a whole porcine aorta subjected to tensile loading using optical coherence tomography–digital volume correlation,” *Front. Mech. Eng.*, vol. 4, p. 3, 2018.
- [59] M. Ang, A. Konstantopoulos, G. Goh, H. M. Htoon, X. Seah, N. C. Lwin, X. Liu, S. Chen, L. Liu, and J. S. Mehta, “Evaluation of a micro-optical coherence tomography for the corneal endothelium in an animal model,” *Sci. Rep.*, vol. 6, p. 29769, 2016.
- [60] K. P. Dingemans, N. Jansen, and A. E. Becker, “Ultrastructure of the normal human aortic media,” *Virchows Arch. A Pathol. Anat. Histol.*, vol. 392, no. 2, pp. 199–216, Jul. 1981.
- [61] T. Okuno, M. Yamaguchi, T. Okada, T. Takahashi, N. Nakamoto, E. Ueshima, K. Sugimura, and K. Sugimoto, “Endovascular creation of aortic dissection in a swine model with technical considerations,” *J. Vasc. Surg.*, vol. 55, no. 5, pp. 1410–1418, 2012.
- [62] C. Martin, T. Pham, and W. Sun, “Significant differences in the material properties between aged human and porcine aortic tissues,” *Eur. J. Cardiothorac. Surg.*, vol. 40, no. 1, pp. 28–34, 2011.
- [63] M. W. Carson and M. R. Roach, “The strength of the aortic media and its role in the propagation of aortic dissection,” *J. Biomech.*, vol. 23, no. 6, pp. 579–588, Jan. 1990.
- [64] I. M. Tiessen and M. R. Roach, “Factors in the initiation and propagation of aortic dissections in human autopsy aortas,” *J. Biomech. Eng.*, vol. 115, no. 1, p. 123, 1993.
- [65] M. R. Roach and S. H. Song, “Variations in strength of the porcine aorta as a function of location,” *Clin. Invest. Med.*, vol. 17, no. 4, pp. 308–318, Aug. 1994.
- [66] A. S. Tam, M. Catherine Sapp, and M. R. Roach, “The effect of tear depth on the propagation of aortic dissections in isolated porcine thoracic aorta,” *J. Biomech.*, vol. 31, no. 7, pp. 673–676, Jul. 1998.
- [67] G. Sommer, T. C. Gasser, P. Regitnig, M. Auer, and G. A. Holzapfel, “Dissection properties of the human aortic media: an experimental study,” *J. Biomech. Eng.*, vol. 130, no. 2, p. 021007, 2008.
- [68] G. Sommer, S. Sherifova, P. J. Oberwalder, O. E. Dapunt, P. A. Ursomanno, A. DeAnda, B. E. Griffith, and G. A. Holzapfel, “Mechanical strength of aneurysmatic and dissected human thoracic aortas at different shear loading modes,” *J. Biomech.*, vol. 49, no. 12, pp. 2374–2382, Aug. 2016.
- [69] X. Leng, B. Zhou, X. Deng, L. Davis, S. M. Lessner, M. A. Sutton, and T. Shazly, “Experimental and numerical studies of two arterial wall delamination modes,” *J. Mech. Behav. Biomed. Mater.*, vol. 77, pp. 321–330, 2018.
- [70] J. Tong, G. Sommer, P. Regitnig, and G. A. Holzapfel, “Dissection properties and mechanical strength of tissue components in human carotid bifurcations,” *Ann. Biomed. Eng.*, vol. 39, no. 6, pp. 1703–1719, Jun. 2011.
- [71] S. Pasta, J. A. Phillipi, T. G. Gleason, and D. A. Vorp, “Effect of aneurysm on the mechanical dissection properties of the human ascending thoracic aorta,” *J. Thorac. Cardiovasc. Surg.*, vol. 143, no. 2, pp. 460–467, Feb. 2012.
- [72] J. A. Phillipi, B. R. Green, M. A. Eskay, M. P. Kotlarczyk, M. R. Hill, A. M. Robertson, S. C. Watkins, D. A. Vorp, and T. G. Gleason, “Mechanism of aortic medial matrix remodeling is distinct in patients with bicuspid aortic valve,” *J. Thorac. Cardiovasc. Surg.*, vol. 147, no. 3, pp. 1056–1064, 2014.
- [73] J. E. Pichamuthu, J. A. Phillipi, D. A. Cleary, D. W. Chew, J. Hempel, D. A. Vorp, and T. G. Gleason, “Differential tensile strength and collagen composition in ascending aortic aneurysms by aortic valve phenotype,” *Ann. Thorac. Surg.*, vol. 96, no. 6, pp. 2147–2154, 2013.
- [74] M. J. Collins, V. Dev, B. H. Strauss, P. W. Fedak, and J. Butany, “Variation in the histopathological features of patients with ascending aortic aneurysms: a study of 111 surgically excised cases,” *J. Clin. Pathol.*, vol. 61, no. 4, pp. 519–523, 2008.
- [75] C. Noble, N. Smulders, R. Lewis, M. J. Carré, S. E. Franklin, S. MacNeil, and Z. A. Taylor, “Controlled peel testing of a model tissue for diseased aorta,” *J. Biomech.*, vol. 49, no. 15, pp. 3667–3675, Nov. 2016.
- [76] P. P. Purslow, “Positional variations in fracture toughness, stiffness and strength of descending thoracic pig aorta,” *J. Biomech.*, vol. 16, no. 11, pp. 947–953, 1983.
- [77] J. Vossoughi and A. Tozeren, “Determination of an effective shear modulus of aorta,” *Russian J. Biomech.*, no. 1-2, pp. 20–35, 1998.
- [78] V. Kas'yanov, B. Purinya, and E. Tseders, “Determination of the shear modulus of human blood-vessel walls,” *Polymer Mechanics*, vol. 14, no. 5, pp. 753–755, 1978.
- [79] X. Lu, J. Yang, J. B. Zhao, H. Gregersen, and G. S. Kassab, “Shear modulus of porcine coronary artery: contributions of media and adventitia,” *Am. J. Physiol. Heart Circ. Physiol.*, vol. 285, no. 5, pp. H1966–H1975, Nov. 2003.
- [80] H. W. Haslach, L. N. Leahy, P. Fathi, J. M. Barrett, A. E. Heyes, T. A. Dumsha, and E. L. McMahon, “Crack propagation and its shear mechanisms in the bovine descending aorta,” *Cardiovasc. Eng. Technol.*, vol. 6, no. 4, pp. 501–518, Dec. 2015.
- [81] H. W. Haslach, P. Riley, and A. Molotsky, “The influence of medial substructures on rupture in bovine aortas,” *Cardiovasc. Eng. Technol.*, vol. 2, no. 4, pp. 372–387, Dec. 2011.
- [82] H. W. Haslach Jr, A. Siddiqui, A. Weerasooriya, R. Nguyen, J. Rosghadol, N. Monforte, and E. McMahon, “Fracture mechanics of shear crack propagation and dissection in the healthy bovine descending aortic media,” *Acta Biomater.*, vol. 68, pp. 53–66, 2018.
- [83] C. M. Witzenburg, R. Y. Dhume, S. B. Shah, C. E. Korenczuk, H. P. Wagner, P. W. Alford, and V. H. Barocas, “Failure of the porcine ascending aorta: multidirectional experiments and a

- unifying microstructural model," *J. Biomech. Eng.*, vol. 139, no. 3, p. 031005, Jan. 2017.
- [84] J. W. Chung, C. Elkins, T. Sakai, N. Kato, T. Vestring, C. P. Semba, S. M. Slonim, and M. D. Dake, "True-lumen collapse in aortic dissection," *Radiology*, vol. 214, no. 1, pp. 87–98, Jan. 2000.
- [85] T. T. Tsai, M. S. Schlicht, K. Khanafer, J. L. Bull, D. T. Valassis, D. M. Williams, R. Berguer, and K. A. Eagle, "Tear size and location impacts false lumen pressure in an ex vivo model of chronic type B aortic dissection," *J. Vasc. Surg.*, vol. 47, no. 4, pp. 844–851, Apr. 2008.
- [86] T. Dziodzio, A. Juraszek, D. Reineke, H. Jenni, E. Zermatten, D. Zimpfer, M. Stoiber, V. Scheikl, H. Schima, M. Grimm, and M. Czerny, "Experimental acute type B aortic dissection: different sites of primary entry tears cause different ways of propagation," *Ann. Thorac. Surg.*, vol. 91, no. 3, pp. 724–727, Mar. 2011.
- [87] E. M. Faure, L. Canaud, P. Cathala, I. Serres, C. Marty-Ané, and P. Alric, "Human ex-vivo model of Stanford type B aortic dissection," *J. Vasc. Surg.*, vol. 60, no. 3, pp. 767–775, Sep. 2014.
- [88] S. V. Peelukhana, Y. Wang, Z. Berwick, J. Kratzberg, J. Krieger, B. Roeder, R. E. Cloughs, A. Hsiao, S. Chambers, and G. S. Kassab, "Role of pulse pressure and geometry of primary entry tear in acute type B dissection propagation," *Ann. Biomed. Eng.*, vol. 45, no. 3, pp. 592–603, Mar. 2017.
- [89] E. K. Prokop, R. F. Palmer, and M. W. Wheat, "Hydrodynamic forces in dissecting aneurysms. In-vitro studies in a Tygon model and in dog aortas," *Circ. Res.*, vol. 27, no. 1, pp. 121–127, Jul. 1970.
- [90] C. van Baardwijk and M. R. Roach, "Factors in the propagation of aortic dissections in canine thoracic aortas," *J. Biomech.*, vol. 20, no. 1, pp. 67–73, Jan. 1987.
- [91] C. Disney, P. Lee, J. Hoyland, M. Sherratt, and B. Bay, "A review of techniques for visualising soft tissue microstructure deformation and quantifying strain Ex Vivo," *J. Microsc.*, 2018.
- [92] F. B. de la Cuesta, R. J. Bean, C. McCallion, K. Wallace, L. Bozec, J. C. Hiller, N. J. Terrill, and I. K. Robinson, "Collagen imaged by coherent x-ray diffraction: towards a complementary tool to conventional scanning SAXS," *J. Phys. Conf. Ser.*, vol. 247, no. 1, p. 012004, 2010.
- [93] M. R. Hee, J. A. Izatt, E. A. Swanson, D. Huang, J. S. Schuman, C. P. Lin, C. A. Puliafito, and J. G. Fujimoto, "Optical coherence tomography of the human retina," *Arch. Ophthalmol.*, vol. 113, no. 3, pp. 325–332, 1995.
- [94] J. Fu, F. Pierron, and P. D. Ruiz, "Elastic stiffness characterization using three-dimensional full-field deformation obtained with optical coherence tomography and digital volume correlation," *J. Biomed. Opt.*, vol. 18, no. 12, p. 121512, 2013.
- [95] S. A. Boppart, B. E. Bouma, C. Pitris, J. F. Southern, M. E. Brezinski, and J. G. Fujimoto, "In vivo cellular optical coherence tomography imaging," *Nat. Med.*, vol. 4, no. 7, pp. 861–865, 1998.
- [96] W. Drexler, U. Morgner, F. Kärtner, C. Pitris, S. Boppart, X. Li, E. Ippen, and J. Fujimoto, "In vivo ultrahigh-resolution optical coherence tomography," *Opt. Lett.*, vol. 24, no. 17, pp. 1221–1223, 1999.
- [97] L. Liu, J. A. Gardecki, S. K. Nadkarni, J. D. Toussaint, Y. Yagi, B. E. Bouma, and G. J. Tearney, "Imaging the subcellular structure of human coronary atherosclerosis using micro-optical coherence tomography," *Nat. Med.*, vol. 17, no. 8, p. 1010, 2011.
- [98] J. Ferruzzi, S.-I. Murtada, G. Li, Y. Jiao, S. Uman, M. Y. Ting, G. Tellides, and J. D. Humphrey, "Pharmacologically improved contractility protects against aortic dissection in mice with disrupted transforming growth factor- β signaling despite compromised extracellular matrix properties," *Arterioscler. Thromb. Vasc. Biol.*, pp. ATVBHA–116, 2016.
- [99] A. J. Schriefl, H. Wolinski, P. Regitnig, S. D. Kohlwein, and G. A. Holzapfel, "An automated approach for three-dimensional quantification of fibrillar structures in optically cleared soft biological tissues," *J. R. Soc. Interface*, vol. 10, no. 80, p. 20120760, 2013.
- [100] W. Krasny, C. Morin, H. Magoariec, and S. Avril, "A comprehensive study of layer-specific morphological changes in the microstructure of carotid arteries under uniaxial load," *Acta Biomater.*, vol. 57, pp. 342–351, 2017.
- [101] S. Pasta, J. A. Phillipi, A. Tsamis, A. D'Amore, G. M. Raffa, M. Pilato, C. Scardulla, S. C. Watkins, W. R. Wagner, T. G. Gleason, and D. A. Vorp, "Constitutive modeling of ascending thoracic aortic aneurysms using microstructural parameters," *Med. Eng. Phys.*, vol. 38, no. 2, pp. 121–130, Feb. 2016.
- [102] J. López-Guimet, J. Andilla, P. Loza-Alvarez, and G. Egea, "High-Resolution Morphological Approach to Analyse Elastin Laminae Injuries of the Ascending Aorta in a Murine Model of Marfan Syndrome," *Sci. Rep.*, vol. 7, May 2017.
- [103] M.-J. Chow, R. Turcotte, C. P. Lin, and Y. Zhang, "Arterial extracellular matrix: a mechanobiological study of the contributions and interactions of elastin and collagen," *Biophys. J.*, vol. 106, no. 12, pp. 2684–2692, 2014.
- [104] J. Schrauwen, A. Vilanova, R. Rezakhanha, N. Stergiopoulos, F. Van De Vosse, and P. Bovendeerd, "A method for the quantification of the pressure dependent 3D collagen configuration in the arterial adventitia," *J. Struct. Biol.*, vol. 180, no. 2, pp. 335–342, 2012.
- [105] R. Wang, L. P. Brewster, and R. L. Gleason Jr, "In-situ characterization of the uncrimping process of arterial collagen fibers using two-photon confocal microscopy and digital image correlation," *J. Biomech.*, vol. 46, no. 15, pp. 2726–2729, 2013.
- [106] I. Costantini, R. Cicchi, L. Silvestri, F. Vanzi, and F. S. Pavone, "In-vivo and ex-vivo optical clearing methods for biological tissues," *Biomed. Opt. Express*, vol. 10, no. 10, pp. 5251–5267, 2019.
- [107] A. Daugherty and L. A. Cassis, "Mouse Models of Abdominal Aortic Aneurysms," *Arterioscler. Thromb. Vasc. Biol.*, vol. 24, no. 3, pp. 429–434, Mar. 2004.
- [108] B. Trachet, L. Aslanidou, A. Piersigilli, R. A. Fraga-Silva, J. Sordet-Dessimo, P. Villanueva-Perez, M. F. Stampanoni, N. Stergiopoulos, and P. Segers, "Angiotensin II infusion into ApoE-/- mice: a model for aortic dissection rather than abdominal aortic aneurysm?" *Cardiovasc. Res.*, vol. 113, no. 10, pp. 1230–1242, Aug. 2017.
- [109] B. Trachet, A. Piersigilli, R. A. Fraga-Silva, L. Aslanidou, J. Sordet-Dessimo, A. Astolfo, M. F. M. Stampanoni, P. Segers, and N. Stergiopoulos, "Ascending aortic aneurysm in angiotensin II-infused mice: formation, progression, and the role of focal dissections," *Arterioscler. Thromb. Vasc. Biol.*, vol. 36, no. 4, pp. 673–681, Apr. 2016.
- [110] D.-S. Jiang, X. Yi, X.-H. Zhu, and X. Wei, "Experimental in vivo and ex vivo models for the study of human aortic dissection: promises and challenges," *Am. J. Transl. Res.*, vol. 8, no. 12, pp. 5125–5140, Dec. 2016.
- [111] W. Ren, Y. Liu, X. Wang, L. Jia, C. Piao, F. Lan, and J. Du, " β -aminopropionitrile monofumarate induces thoracic aortic dissection in c57bl/6 mice," *Sci. Rep.*, vol. 6, p. 28149, 2016.
- [112] G. Logghe, B. Trachet, L. Aslanidou, P. Villanueva-Perez, J. De Backer, N. Stergiopoulos, M. Stampanoni, H. Aoki, and P. Segers, "Propagation-based phase-contrast synchrotron imaging of aortic dissection in mice: from individual elastic lamella to 3D analysis," *Sci. Rep.*, vol. 8, no. 1, Dec. 2018.
- [113] D. M. Milewicz and F. Ramirez, "Therapies for thoracic aortic aneurysms and acute aortic dissections: old controversies and new opportunities," 2019.
- [114] D. M. Milewicz, S. K. Prakash, and F. Ramirez, "Therapeutics targeting drivers of thoracic aortic aneurysms and acute aortic dissections: insights from predisposing genes and mouse models," *Annu. Rev. Med.*, vol. 68, pp. 51–67, 2017.
- [115] M. K. Razavi, E. Nishimura, S. Slonim, W. Zeigler, S. Kee, H. L. Witherall, C. P. Semba, and M. D. Dake, "Percutaneous creation of acute type-B aortic dissection: an experimental model for endoluminal therapy," *J. Vasc. Interv. Radiol.*, vol. 9, no. 4, pp. 626–632, Jul. 1998.
- [116] H. Terai, N. Tamura, S. Yuasa, T. Nakamura, Y. Shimizu, and M. Komeda, "An experimental model of Stanford type B aortic dissection," *J. Vasc. Interv. Radiol.*, vol. 16, no. 4, pp. 515–519, Apr. 2005.

- [117] C.-H. Marty-Ané, O. SerreCousiné, J.-C. Laborde, V. Costes, H. Mary, and J.-P. Senac, "Use of a Balloon-expandable Intravascular Graft in the Management of Type B Aortic Dissection in an Animal Model," *J. Vasc. Interv. Radiol.*, vol. 6, no. 1, pp. 97–103, Jan. 1995.
- [118] D. L. S. Morales, J. A. Quin, J. H. Braxton, G. L. Hammond, R. J. Gusberg, and J. A. Elefteriades, "Experimental confirmation of effectiveness of fenestration in acute aortic dissection," *Ann. Thorac. Surg.*, vol. 66, no. 5, pp. 1679–1683, Nov. 1998.
- [119] M. Thubrikar, P. Agali, and F. Robicsek, "Wall stress as a possible mechanism for the development of transverse intimal tears in aortic dissections," *J. Med. Eng. Technol.*, vol. 23, no. 4, pp. 127–134, 1999.
- [120] C. J. Beller, M. R. Labrosse, M. J. Thubrikar, and F. Robicsek, "Finite element modeling of the thoracic aorta: including aortic root motion to evaluate the risk of aortic dissection," *J. Med. Eng. Technol.*, vol. 32, no. 2, pp. 167–170, Jan. 2008.
- [121] D. P. Nathan, C. Xu, J. H. Gorman, R. M. Fairman, J. E. Bavaria, R. C. Gorman, K. B. Chandran, and B. M. Jackson, "Pathogenesis of acute aortic dissection: a finite element stress analysis," *Ann. Thorac. Surg.*, vol. 91, no. 2, pp. 458–463, Feb. 2011.
- [122] C. Cavinato, J. Molimard, N. Curt, S. Campisi, L. Orgéas, and P. Badel, "Does the knowledge of the local thickness of human ascending thoracic aneurysm walls improve their mechanical analysis?" *Front. Bioeng. Biotechnol.*, vol. 7, p. 169, 2019.
- [123] T. C. Gasser and G. A. Holzapfel, "Modeling the propagation of arterial dissection," *Eur. J. Mech. A. Solids*, vol. 25, no. 4, pp. 617–633, Jul. 2006.
- [124] A. Ferrara and A. Pandolfi, "A numerical study of arterial media dissection processes," *Int. J. Fract.*, vol. 166, no. 1-2, pp. 21–33, Nov. 2010.
- [125] A. Ferrara and A. Pandolfi, "Numerical modelling of fracture in human arteries," *Comput. Methods Biomed. Eng. Imaging Vis.*, vol. 11, no. 5, pp. 553–567, 2008.
- [126] J. Brunet, B. Pierrat, E. Maire, J. Adrien, and P. Badel, "A combined experimental-numerical lamellar-scale approach of tensile rupture in arterial medial tissue using x-ray tomography," *J. Mech. Behav. Biomed. Mater.*, vol. 95, pp. 116–123, 2019.
- [127] L. Wang, S. M. Roper, N. A. Hill, and X. Luo, "Propagation of dissection in a residually-stressed artery model," *Biomech. Model. Mechanobiol.*, vol. 16, no. 1, pp. 139–149, Feb. 2017.
- [128] L. Wang, S. M. Roper, X. Y. Luo, and N. A. Hill, "Modelling of tear propagation and arrest in fibre-reinforced soft tissue subject to internal pressure," *J. Eng. Math.*, vol. 95, no. 1, pp. 249–265, Dec. 2015.
- [129] L. Wang, N. A. Hill, S. M. Roper, and X. Luo, "Modelling peeling-and pressure-driven propagation of arterial dissection," *J. Eng. Math.*, vol. 109, no. 1, pp. 227–238, 2018.
- [130] S. Roccabianca, C. Bellini, and J. Humphrey, "Computational modelling suggests good, bad and ugly roles of glycosaminoglycans in arterial wall mechanics and mechanobiology," *J. R. Soc. Interface*, vol. 11, no. 97, p. 20140397, 2014.
- [131] S. B. Shah, C. Witzenburg, M. F. Hadi, H. P. Wagner, J. M. Goodrich, P. W. Alford, and V. H. Barocas, "Prefailure and failure mechanics of the porcine ascending thoracic aorta: experiments and a multiscale model," *J. Biomech. Eng.*, vol. 136, no. 2, p. 021028, Feb. 2014.
- [132] J. R. Thunes, S. Pal, R. N. Fortunato, J. A. Phillipi, T. G. Gleason, D. A. Vorp, and S. Maiti, "A structural finite element model for lamellar unit of aortic media indicates heterogeneous stress field after collagen recruitment," *J. Biomech.*, vol. 49, no. 9, pp. 1562–1569, Jun. 2016.
- [133] J. R. Thunes, J. A. Phillipi, T. G. Gleason, D. A. Vorp, and S. Maiti, "Structural modeling reveals microstructure-strength relationship for human ascending thoracic aorta," *J. Biomech.*, vol. 71, pp. 84–93, Apr. 2018.
- [134] S. Pal, A. Tsamis, S. Pasta, A. D'Amore, T. G. Gleason, D. A. Vorp, and S. Maiti, "A mechanistic model on the role of "radially-running" collagen fibers on dissection properties of human ascending thoracic aorta," *J. Biomech.*, vol. 47, no. 5, pp. 981–988, Mar. 2014.
- [135] P. T. O'Gara and R. W. DeSanctis, "Acute aortic dissection and its variants: toward a common diagnostic and therapeutic approach," *Circulation*, vol. 92, no. 6, pp. 1376–1378, 1995.
- [136] C. A. Nienaber and R. E. Clough, "Management of acute aortic dissection," *The Lancet*, vol. 385, no. 9970, pp. 800–811, 2015.
- [137] A. Emmott, I. El-Hamamsy, and R. L. Leask, "Histopathological and biomechanical properties of the aortic wall in 2 patients with chronic type A aortic dissection," *Cardiovasc. Pathol.*, vol. 29, pp. 48–52, Jul. 2017.
- [138] Z. Bai, J. Gu, Y. Shi, and W. Meng, "Effect of inflammation on the biomechanical strength of involved aorta in type a aortic dissection and ascending thoracic aortic aneurysm: an initial research," *Anatol. J. Cardiol.*, vol. 20, no. 2, pp. 85–92, 2018.
- [139] F. Luo, X.-L. Zhou, J.-J. Li, and R.-T. Hui, "Inflammatory response is associated with aortic dissection," *Ageing Res. Rev.*, vol. 8, no. 1, pp. 31–35, 2009.
- [140] D. M. Milewicz, D.-C. Guo, V. Tran-Fadulu, A. L. Lafont, C. L. Papke, S. Inamoto, C. S. Kwartler, and H. Pannu, "Genetic basis of thoracic aortic aneurysms and dissections: focus on smooth muscle cell contractile dysfunction," *Annu. Rev. Genomics Hum. Genet.*, vol. 9, pp. 283–302, 2008.
- [141] Y. von Kodolitsch, S. K. Csósz, D. H. Koschyk, I. Schalwat, R. Loose, M. Karck, C. Dieckmann, R. Fattori, A. Haverich, J. Berger et al., "Intramural hematoma of the aorta: predictors of progression to dissection and rupture," *Circulation*, vol. 107, no. 8, pp. 1158–1163, 2003.
- [142] L. Hiratzka, G. Bakris, J. Beckman, R. Bersin, V. Carr, D. Casey, K. Eagle, L. Hermann, E. Isseibacher, E. Kazerooni et al., "Guidelines for the diagnosis and management of patients with thoracic aortic disease: a report of the american college of cardiology foundation/american heart association task force on practice guidelines, american association for thoracic surgery, american college of radiology, american stroke association, society of cardiovascular anesthesiologists, society for cardiovascular angiography and interventions, society of interventional radiology, society of thoracic surgeons, and society for vascular medicine," *Circulation*, vol. 121, no. 3, pp. e266–e369, 2010.
- [143] I. Gore, "Pathogenesis of dissecting aneurysm of the aorta," *Arch. Pathol.*, vol. 53, no. 2, pp. 142–153, 1952.
- [144] A. E. Hirst, V. J. Johns, and S. W. Kime, "Dissecting aneurysm of the aorta: a review of 505 cases," *Medicine (Baltimore)*, vol. 37, no. 3, p. 217, 1958.
- [145] R. Erbel, H. Oelert, J. Meyer, M. Puth, S. Mohr-Katoly, D. Hausmann, W. Daniel, S. Maffei, A. Caruso, and F. E. Covino, "Effect of medical and surgical therapy on aortic dissection evaluated by transesophageal echocardiography. implications for prognosis and therapy. the european cooperative study group on echocardiography," *Circulation*, vol. 87, no. 5, pp. 1604–1615, 1993.
- [146] S. Mohr-Kahaly, R. Epbel, P. Kearney, M. Puth, and J. Meyer, "Aortic intramural hemorrhage visualized by transesophageal echocardiography: findings and prognostic implication," *J. Am. Coll. Cardiol.*, vol. 23, no. 3, pp. 658–664, 1994.
- [147] H. Shimizu, H. Yoshino, H. Udagawa, A. Watanuki, K. Yano, H. Ide, K. Sudo, and K. Ishikawa, "Prognosis of aortic intramural hemorrhage compared with classic aortic dissection," *Am. J. Cardiol.*, vol. 85, no. 6, pp. 792–5, 2000.
- [148] R. J. Zotz, R. Erbel, and J. Meyer, "Noncommunicating intramural hematoma: an indication of developing aortic dissection?" *J. Am. Soc. Echocardiogr.*, vol. 4, no. 6, pp. 636–638, 1991.
- [149] S. Gasperini, V. Zacà, and S. Mondillo, "Real-time imaging of dissection of the ascending aorta," *Eur. J. Echocardiogr.*, vol. 9, no. 1, pp. 97–98, 2007.
- [150] C. I. Stefanidis, P. E. Karayannacos, H. K. Boudoulas, C. G. Stratos, C. V. Vlachopoulos, I. A. Dontas, and P. K. Toutouzas, "Medial necrosis and acute alterations in aortic distensibility following removal of the vasa vasorum of canine

- ascending aorta,” *Cardiovasc. Res.*, vol. 27, no. 6, pp. 951–956, 1993.
- [151] D. Angouras, D. P. Sokolis, T. Dosios, N. Kostomitsopoulos, H. Boudoulas, G. Skalkeas, and P. E. Karayannacos, “Effect of impaired vasa vasorum flow on the structure and mechanics of the thoracic aorta: implications for the pathogenesis of aortic dissection,” *Eur. J. Cardiothorac. Surg.*, vol. 17, no. 4, pp. 468–473, Apr. 2000.
- [152] J. Tong, Y. Cheng, and G. A. Holzapfel, “Mechanical assessment of arterial dissection in health and disease: advancements and challenges,” *J. Biomech.*, vol. 49, no. 12, pp. 2366–2373, Aug. 2016.
- [153] J. L. Zitnay, Y. Li, Z. Qin, B. H. San, B. Depalle, S. P. Reese, M. J. Buehler, S. M. Yu, and J. A. Weiss, “Molecular level detection and localization of mechanical damage in collagen enabled by collagen hybridizing peptides,” *Nat. Commun.*, vol. 8, p. 14913, 2017.
- [154] M. I. Converse, R. G. Walther, J. T. Ingram, Y. Li, S. M. Yu, and K. L. Monson, “Detection and characterization of molecular-level collagen damage in overstretched cerebral arteries,” *Acta Biomater.*, vol. 67, pp. 307–318, 2018.
- [155] M. Marino, M. I. Converse, K. L. Monson, and P. Wriggers, “Molecular-level collagen damage explains softening and failure of arterial tissues: A quantitative interpretation of chp data with a novel elasto-damage model,” *J. Mech. Behav. Biomed. Mater.*, vol. 97, pp. 254–271, 2019.